SDI
SYSTEM DYNAMICS INCORPORATED

INTERIM FINAL TECHNICAL REPORT

for

SPACE SHUTTLE PROPULSION PARAMETER ESTIMATION USING OPTIMAL ESTIMATION TECHNIQUES

VOLUME I

CONTRACT NO. NAS8-35324

submitted to

NATIONAL AERONAUTICS AND SPACE ADMINISTRATION

MARSHALL SPACE FLIGHT CENTER

HUNTSVILLE, ALABAMA

19 November 1983

1219 N.W. 10 AVE. • POST OFFICE BOX 13687
GAINESVILLE, FLORIDA 32604 • (904)-376-3199

INDEX

1.0 INTRODUCTION

This report summarizes the mathematical developments and their computer program implementation for the Space Shuttle propulsion parameter estimation project. The estimation approach chosen is the extended Kalman filtering with a modified Bryson-Frazier smoother. This estimation technique has been used on previous aerodynamic coefficient parameter estimation efforts. Its use here is motivated by the objective of obtaining better estimates than those available from filtering and to eliminate the lag associated with filtering.

The estimation technique uses as the dynamical process the six degree equations-of-motion resulting in twelve state vector elements. In addition to these are mass and solid propellant burn depth as the "system" state elements. The "parameter" state elements can include aerodynamic coefficient, inertia, center-of-gravity, atmospheric wind, etc. deviations from referenced values. Propulsion parameter state elements have been included not as options just discussed but as the main parameter states to be estimated. The mathematical developments have been completed for all these parameters. Since the systems dynamics and measurement processes are non-linear functions of the states, the mathematical developments are taken up almost entirely by the linearization of these equations as required by the estimation algorithms.

This estimation approach has the objective of using all available measurements. These measurements include ground based radar tracking, on-board inertially stabilized platform accelerometer and attitude data, SSME pressurants/fuel flow rates and power level, and SRB head pressure.

The estimation algorithm is implemented to process each of these measurements separately with the assumption that the errors associated with these measurements are uncorrelated.

The computer programs have been developed in a highly modular structure to facilitate understanding, checkout and, if necessary, modification. The computer programs reside on NASA's VAX 1 computer system in the HOSC facility. Approximately eighty separate routines have been developed to implement this estimation technique. As specified by the ITYPE variable, the FILTER program can provide three modes of data processing. These include: ITYPE = 0 to generate synthetic measurement data, ITYPE = 1 to provide optimal estimates based on the extended Kalman filter algorithm, and ITYPE > 1 to propagate the state error covariance matrix with no updating from the measurement process. The SMOOTH program provides estimates of the system and parameter state elements from the filter estimates provided as input.

Preliminary results indicate that the propulsion parameters strongly affect the states and associated measurements. The resulting estimates should be rapidly converged upon by the filter algorithm and accuracy improved upon by the smoother algorithm. These preliminary results will be discussed later in this report.

This report, Volume I, is organized as the following. In Section 2.0 the filtering and smoothing algorithms are presented. Section 3.0 contains the system and parameter state models, their linearization, the measurement equations, and their linearization with respect to the state elements. The computer programs are described in Section 4.0 along with some preliminary results. Appendices A, B and C contain auxiliary partial derivatives (linearizations) and Appendix D contains the aerodynamic coefficient model

and data used as the referenced model in the estimation program. Volume II contains the computer listings of the FILTER and SMOOTH programs with associated example input and output data listings.

2.0 FILTERING AND SMOOTHING ALGORITHM

The Space Shuttle Parameter Estimation Program utilizes optimal estimation techniques to provide estimates of the propulsion system parameters. The technique selected is the extended Kalman filter and the modified Bryson-Frazier smoother. By modeling the propulsion system parameters as time correlated random variables, improved estimates of these parameters are obtained and are properly time phased by removing the filter induced lag by using the combined filter/smoother. The smoother also provides improved estimates of the initial state estimates.

The system, in state-space notation, is modeled as the continuous dynamical system disturbed by additive Gaussian white noise

$$\dot{\underline{x}} = \underline{f}(\underline{x}(t), t) + G(t)\, \underline{w}(t) + \underline{u}(t), \quad \underline{x}(o) = \underline{x}_o \tag{1}$$

where

$\underline{x}$ = n-dimensional state vector

$\underline{x}_o$ = Gaussian initial condition vector with covariance P_o

$\underline{w}(t)$ = p-dimensional white, zero-mean white Gaussian noise with covariance

$$E[\underline{w}(t)\, \underline{w}^T(\tau)] = Q(t)\, \delta(t - \tau)$$

$\underline{u}(t)$ = n-dimensional control vector.

The elements of the vector $\underline{x}(t)$ represent vehicle position, velocities, attitudes, angular rates, aerodynamic and propulsion parameters, measurement biases, etc. Elements of $\underline{u}(t)$ include known control inputs such as SSME power level commands.

The system described by equation (1) is observed at discrete times, t_k, with not all states being directly measured. Some measurements are non-linear functions of the elements of the state vector $\underline{x}(t)$. In general the measurement process is described as

$$\underline{z}_k = \underline{h}_k(\underline{x}(t_k)) + \underline{v}_k \tag{2}$$

where

$\underline{z}_k$ = m-dimensional observation vector

$\underline{h}_k$ = functional representation of the measurements in terms of the states

$\underline{v}_k$ = m-dimensional, zero-mean, while Gaussian noise sequence with covariance

$$E[\underline{v}_i \, \underline{v}_j^T] = R_i \, \delta_{i,j}$$

Examples of the elements of the observation vector $\underline{z}_k$ include radar measurements of range, azimuth, and elevation from the radar site to the vehicle.

It is assumed that the system process noise vector $\underline{w}(t)$ and the measurement noise vector $\underline{v}_k$ are uncorrelated. Also, the system state initial condition vector $\underline{x}_o$ is not correlated with either of these two noise vectors. Therefore

$$E[\underline{w}(t) \, \underline{v}_k^T] = 0, \quad E[w(t) \, \underline{x}_o^T] = 0, \quad E[\underline{x}_o \, \underline{v}_k^T] = 0$$

where the superscript T denotes transpose. For later reference, the following matricies are defined

$$F(\underline{x}(t), t) = \frac{\partial \underline{f}(\underline{x}(t), t)}{\partial \underline{x}(t)} \tag{3}$$

and

$$H(\underline{x}_k(-)) = \frac{\partial \underline{h}(\underline{x}(t_k))}{\partial \underline{x}(t_k)} \, . \tag{4}$$

These matricies are linearizations of the dynamics and measurement models respectively, evaluated about either a nominal or reference value of the state, or about the state estimate.

2.1 Extended Kalman Filter Algorithm

The extended Kalman filter algorithm is in essence a conventional linear Kalman filter algorithm applied to a mathematical model resulting from the linearization of the system model equation (1), and measurement process, equation (2), about a current state estimate. The filter yields optimal estimates if the linearization is accurate, i.e., the state estimate closely approximates the true state. The derivation of the algorithm can be found in reference [1].

The algorithm proceeds as follows. After initialization of the state estimate and covariance, the state estimate and covariance are propagated forward in time until a measurement update is available, by

$$\dot{\hat{\underline{x}}} = \underline{f}(\hat{\underline{x}}(t), t) \qquad , \qquad t_{k-1} < t \leq t_k \tag{5}$$

and

$$\dot{P}(t) = F(\hat{\underline{x}}(t), t)\, P(t) + P(t)\, F(\hat{\underline{x}}(t), t)^T + G(t)\, Q(t)\, G(t)^T \tag{6}$$

At the measurement time, the state estimate and covariance are updated by

$$\hat{\underline{x}}_k(+) = \hat{\underline{x}}_k(-) + K_k(\underline{z}_k - \underline{h}_k(\hat{\underline{x}}_k(-))) \tag{7}$$

and

$$P_k(+) = (I - K_k H_k(\hat{\underline{x}}_k(-))) P_k(-) \tag{8}$$

where the (-) and (+) represent the appropriate values just before and just after the update. The updated values are used to reinitialize the time propagation equations (3) and (4) for integrating up to the next measurement time. The Kalman gain matrix is computed as

$$K_k = P_k(-) H_k(\hat{\underline{x}}_j(-))^T (H_k(\hat{\underline{x}}_k(-)) P_k(-) H_k(\hat{\underline{x}}_k(-))^T + R_k)^{-1} \tag{9}$$

This algorithm is repeated until the last time point, t_N, is processed. For later use in the smoother algorithm, various combinations of the state estimates ($\hat{\underline{x}}$), measurements ($\underline{z}$), linearized dynamics matrix (F) and measurement matrix (H), measurement noise covariance (R) and estimation error covariance matrix (P) must be stored for each time instant to be processed by the smoother algorithm.

2.2 Modified Bryson-Frazier Smoother Algorithm

The operation of the smoother algorithm is similar to the filter algorithm except in reverse time. The derivation of this smoother algorithm is found in reference [2]. This fixed interval smoothing algorithm provides optimal estimates given all the measurements in comparison to the filtering algorithm providing optimal estimates given the previous

measurements processed. Therefore the smoother provides improved estimates in addition to removing the time lag induced by the filter algorithm.

The smoothing algorithm adjoint variables, $\underline{\lambda}$ and Λ are "initialized" at the final time processed by the filter, T,

$$\underline{\lambda}(T-) = -H_N^T(H_N P_N H_N^T + R_N)^{-1} (\underline{z}_N - \underline{H}_N(\hat{\underline{x}}_N(-))) \delta_{t_{N,T}} \tag{10}$$

and

$$\Lambda(T-) = H_N^T(H_N P_N H_N^T + R_N)^{-1} H_N \delta_{t_{N,T}} \tag{11}$$

If T is not an observation time, $\underline{\lambda}$ and Λ are zero. The adjoint variables are propagated in reverse time to the next previous measurement time by

$$\dot{\underline{\lambda}} = - F(\hat{\underline{x}}(t), t) \underline{\lambda} \qquad , \qquad t_k \leq t < t_{k+1} \tag{12}$$

$$\dot{\Lambda} = - F(\hat{\underline{x}}(t), t)^T \Lambda - \Lambda F(\hat{\underline{x}}(t), t) \tag{13}$$

At the time of an available measurement, t_k, the adjoint variables are updated by

$$\underline{\lambda}(-) = \underline{\lambda}(+) - H_k^T(H_k P_k H_k^T + R_k)^{-1} ((\underline{z}_k - \underline{h}_k(\underline{x}_k(-))) + (H_k P_k H_k^T + R_k) K_k^T \underline{\lambda}(+)) \tag{14}$$

and

$$\Lambda(-) = (I - K_k H_k)^T \Lambda(+) (I - K_k H_k) + H_k^T(H_k P_k H_k^T + R_k)^{-1} H_k \tag{15}$$

The smoother state estimate and error covariance are obtained using the filter estimate and covariance and the adjoint variables by

$$\underline{x}^*(t) = \underline{\hat{x}}(t) - P(t)\ \underline{\lambda}(t) \tag{16}$$

and

$$P^*(t) = P(t) - P(t)\ \Lambda(t)\ P(t). \tag{17}$$

Due to the potential number of time points to be processed, smoother estimates may only be computed at the discrete measurement times. For this approach the propagation equations (10) and (11) are replaced by

$$\underline{\lambda}_k(+) = \Phi_k^T\ \underline{\lambda}(-)_{k+1} \tag{18}$$

and

$$\Lambda_k(+) = \Phi_k^T\ \Lambda_{k+1}(-)\ \Phi_k \tag{19}$$

where Φ_k^T is the state transition matrix formed with the linearized dynamics matrix F to propagate the adjoint variable from time t_{k+1} to time t_k. The algorithm continues in reverse time until the initial time is reached.

2.3 Iterations with the Filter/Smoother Algorithm

The performance of the filter/smoother algorithm is a direct result of the accuracy of the linearization. Repeated operations of the algorithms with adjustments in initial state estimates and covariance in each cycle can yield improved estimates. This technique is known as global iterated

filtering as defined in reference [3]. Each cycle of operating the algorithms would yield increasing improvements in the state estimates.

This feature of the algorithm operation is of special interest to the propulsion parameter estimation problem using the NASA predictive models. Initial, or nominal, values of the parameters of interest can be used to obtain the necessary partial derivatives indicated earlier. From operating the algorithm improved estimates of those parameters are obtained. Using these improved estimates, more accurate partial derivatives are obtained for use in the algorithms. This process is continued until there is in essence no change in the partial derivatives or quality of the state estimates. If the linearization is accurate, the measurement residual should be a white noise process with known covariance.

3.0 FILTER/SMOOTHER ALGORITHM SYSTEM AND MEASUREMENT MODEL

The usefulness of the filter/smoother algorithm is to provide estimates of the system states from the observed motion and dynamics while the system is driven by known and unknown elements. These unknown elements are elements of the system state vector to be estimated. The evolution of motion resulting from these known and unknown elements is assumed to be suitably represented for this study by a six degree-of-freedom (6 DOF) rigid body equations of motion. These equations are presented and discussed in section 3.1.

To implement these equations into the filter/smoother algorithm presented in section 2.0, a linearization of the system state and measurement models is required. These linearized equations are presented in section 3.2.

3.1 Equations of Motion and Measurement Equations

3.1.1 Rigid Body Equations of Motion

The rate of change of vehicle velocity in body coordinates, $\underline{v}^{(B)}$, as a result of external forces acting on the vehicle is described by

$$\dot{\underline{v}}^{(B)} = \frac{\rho A v_m^2}{2m} \underline{c}_f + {}^{B}_{C}I \, \underline{g}^{(\cdot)}(\underline{r}^{(I)}) - \underline{\omega} \times \underline{v}^{(B)} + \frac{\underline{f}_T^{(B)}}{m} + \frac{\underline{f}_P^{(B)}}{m} \qquad (20)$$

where

ρ = atmospheric density

A = aerodynamic coefficient referenced area

v_m = magnitude of vehicle velocity relative to the surrounding air mass

m = vehicle mass

$\underline{c}_f$ = aerodynamic force coefficient vector

$\underline{g}^{(I)}$ $(\underline{r}^{(I)})$ = gravity vector in inertial coordinates

$\underline{\omega}$ = angular rotation of the body relative to the inertial frame

$\underline{f}_T^{(B)}$ = resultant thrust force vector in body coordinates

$\underline{f}_p^{(B)}$ = resultant plume force vector in body coordinates

The rate of change of vehicle position in inertial coordinates, $\underline{r}^{(I)}$, is then obtained by

$$\dot{\underline{r}}^{(I)} = {}^{I}C^{B}\, v^{(B)} \tag{21}$$

where ${}^{I}C^{B}$ is the transformation matrix from body coordinates to inertial coordinates. The elements of the ${}^{I}C^{B}$ transformation matrix are obtained from the resulting Euler angles defined by

$$\begin{bmatrix} \dot{\varphi} \\ \dot{\theta} \\ \dot{\psi} \end{bmatrix} = \begin{bmatrix} 1 & \sin\varphi\tan\theta & \cos\varphi\tan\theta \\ 0 & \cos\varphi & -\sin\varphi \\ 0 & \sin\varphi\sec\theta & \cos\varphi\sec\theta \end{bmatrix} \begin{bmatrix} p \\ q \\ r \end{bmatrix}$$

where φ, θ, and ψ are roll, pitch and yaw attitudes respectively. The roll, pitch and yaw rates of the body relative to inertial coordinates are p, q, and r respectively. Finally, the rate of change of the body rates relative to inertial is given by

$$\dot{\underline{\omega}} = \begin{bmatrix} \dot{p} \\ \dot{q} \\ \dot{r} \end{bmatrix} = [I]^{-1} \left[\frac{\rho A v_m^2}{2} \underline{\ell c}_m + \frac{\rho A v_m^2}{2} (\underline{r}_A^{(B)} - \underline{r}_{cg}^{(B)}) \times \underline{c}_f \right.$$

$$\left. - \underline{\omega} \times (I\underline{\omega}) + \underline{T}_T^{(B)} + \underline{T}_P^{(B)} \right] \qquad (23)$$

where

I = vehicle moments of inertia matrix

$\underline{\ell c}_m$ = aerodynamic coefficient referenced length and moment coefficient vector

$\underline{r}_{cg}^{(B)}$ = vehicle center-of-gravity vector in body coordinates

$\underline{r}_A^{(B)}$ = aerodynamic coefficient reference position in body coordinates

$\underline{T}_T^{(B)}$ = resultant thrust torque vector in body coordinates

$\underline{T}_P^{(B)}$ = resul nt plane torque vector in body coordinates

The equations of motion represent the first twelve elements of the system state vector. These equations are summarized in Table 3.1.1-1.

The moment of inertia matrix I in general is given by

$$I = \begin{bmatrix} I_x & -I_{xy} & -I_{zx} \\ -I_{xy} & I_y & -I_{yz} \\ -I_{zx} & -I_{yz} & I_z \end{bmatrix} \qquad (24)$$

for the moment axis terms, i.e., I_y, and the product of inertia terms, i.e., I_{zx}.

TABLE 3.1.1-1

Equations of Motion

(first twelve system states)

$$\dot{\underline{r}}^{(I)} = {}^{I}_{C}B\ \underline{v}^{(B)} \qquad \text{inertial mean of 50}$$

$$\dot{\underline{v}}^{(B)} = \frac{\rho v_m^2 A}{2m}\underline{c}_f + {}^{B}_{C}I\ \underline{g}^{(I)}(\underline{r}^{(I)}) - \underline{\omega} \times \underline{v}^{(B)} + \frac{\underline{f}_T^{(B)}}{m} + \frac{\underline{f}_P^{(B)}}{m}$$

$$\dot{\underline{\theta}} = \begin{bmatrix} \dot{\varphi} \\ \dot{\theta} \\ \dot{\psi} \end{bmatrix} = \begin{bmatrix} 1 & \sin\varphi\tan\theta & \cos\varphi\tan\theta \\ 0 & \cos\varphi & -\sin\varphi \\ 0 & \sin\varphi\sec\theta & \cos\varphi\sec\theta \end{bmatrix} \begin{bmatrix} p \\ q \\ r \end{bmatrix}$$

$$\dot{{}^{I}\underline{\omega}}^{B} = \begin{bmatrix} \dot{p} \\ \dot{q} \\ \dot{r} \end{bmatrix} = [I]^{-1}\left[\frac{\rho v_m^2 Ad}{2}\underline{c}_m + \frac{\rho v_m^2 A}{2}(\underline{r}_A - \underline{r}_{cg})^{(B)} \times \underline{c}_f - \underline{\omega} \times ([I]\,\underline{\omega}) + \underline{T}_T + \underline{T}_P\right]$$

The aerodynamic force and moment coefficients and plume forces are defined as functions of angle-of-attack, α, and angle-of-sideslip, β, as shown in Figure 3.1.1-1. The body referenced relative velocity vector, removing the wind velocity, $\underline{v}_w$, from the vehicle velocity, is given by

$$\underline{v}_r = \underline{v}^{(B)} - {}^{B}C^{I}\,\underline{v}_w = \underline{v}^{(B)} - {}^{B}C^{LL}\,\underline{v}_w^{(LL)} \tag{25}$$

where $\underline{v}_w^{(LL)}$ is the local-level referenced wind velocity vector. The following equations define α and β in terms of the components of $\underline{v}_r$

$$\alpha = \tan^{-1}\left(\frac{v_{r_3}}{v_{r_1}}\right) \tag{26}$$

$$\beta = \sin^{-1}\left(\frac{v_{r_2}}{v_m}\right) \tag{27}$$

where

$$v_m = \left(v_{r_1}^2 + v_{r_2}^2 + v_{r_3}^2\right)^{\frac{1}{2}} \tag{28}$$

The resultant thrust force $\underline{f}_T^{(B)}$ is expanded as

$$\underline{f}_T^{(B)} = \sum_{i=1}^{n} {}^{B}C_i^{\ell}\begin{bmatrix} f_{T_i}^{\ell} \\ 0 \\ 0 \end{bmatrix} \triangleq \sum_{i=1}^{n} {}^{B}C_i^{\ell}\,\underline{f}_{T_i}^{(\ell)} \tag{29}$$

where the transformation matrix ${}^{B}C_i^{\ell}$ transforms the magnitude of thrust for each thrusting device, $f_{T_i}^{\ell}$, from its center-line to the body coordinates. The general equation for f_{T_i} is

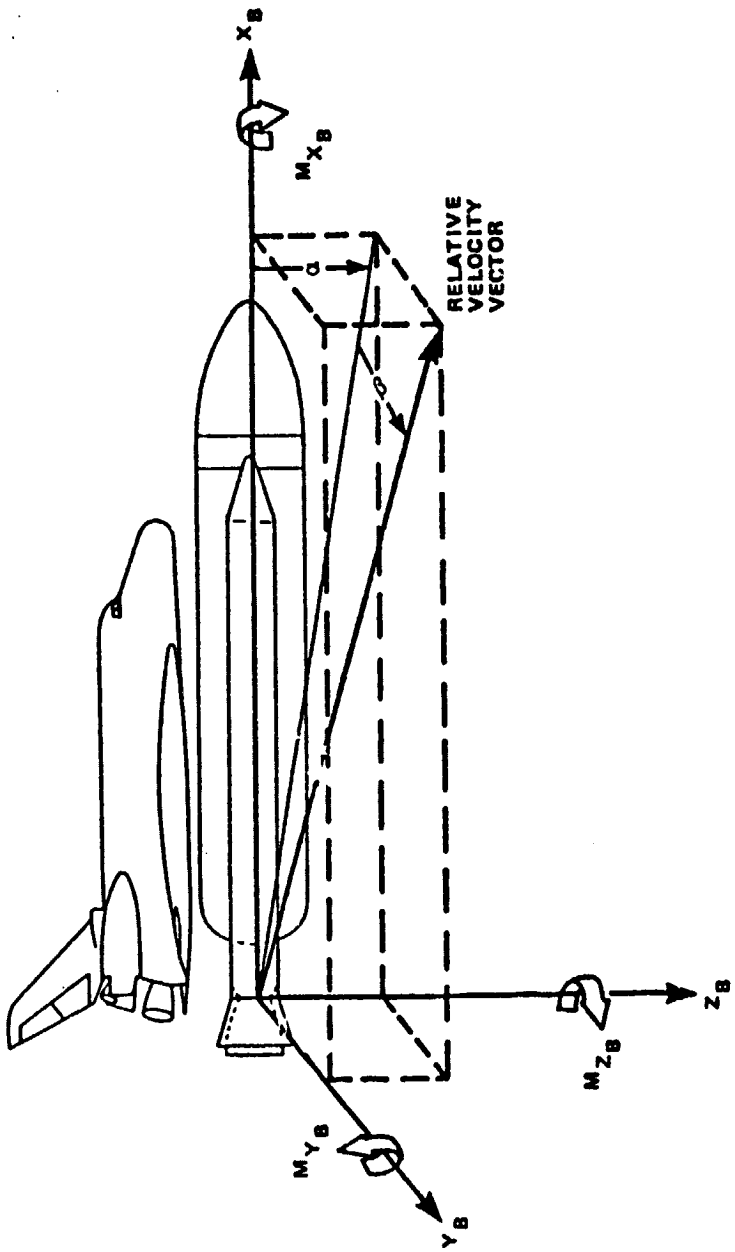

FIGURE 3.1.1-1. Body Referenced Wind Axis System

$$f_{T_i} = f_{T_{ivac}} - P_{s_i} A_e$$

where

$f_{T_{ivac}}$ = vacuum thrust

P_{s_i} = atmospheric pressure at motor exit

A_e = motor exit cone area

The matrix ${}^{B_C}_{i}\mathcal{L}$ is different for the SSME's and SRB's and is given by

$$B_C\mathcal{L}_i = \begin{cases} B_C MP \; MP_C G \; G_C\mathcal{L} & \text{SSME} \\ B_C\mathcal{L} & \text{SRB} \end{cases} \qquad (30)$$

where

$B_C MP$ = transformation from the engine mount plane to the body coordinates

$MP_C G$ = transformation from the gimbal reference plane to mount plane (structural deformation)

$G_C\mathcal{L}$ = transformation from enterline to the gimbal reference plane

$B_C\mathcal{L}$ = transformation from SRB nozzle centerline to the body coordinates (gimbal angles).

The resultant thrust torque is the summation of the torque contribution from each thrusting device and is given by

$$\underline{T}_T^{(B)} = \sum_{i=1}^{n} (\underline{r}_{T_i}^{(B)} - \underline{r}_{cg}^{(B)}) \times {}^{B}C_i^{\mathcal{L}} \begin{bmatrix} f_{T_i}^{\mathcal{L}} \\ 0 \\ 0 \end{bmatrix} \tag{31}$$

where

$\underline{r}_{T_i}^{(B)}$ = body coordinates of the thrust reference point for the i^{th} thrusting device.

3.1.2 Measurement Equations

The measurements assumed available for the filter/smoother algorithm include inertial platform acceleration and attitudes, ground based radar tracking, SRB's head pressure, SSME's chamber pressures, liquid H_2 flow rates, pressurant flow rates. The ET volumetric levels are available; however, due to their limited number (4), they may only be used for alternate checks of the filter/smoother algorithm performance.

The propulsion related measurements will be treated in a separate section. In the following, the inertial platform acceleration measurements, attitude measurements and ground based tracking measurements models will be described for later linearization.

3.1.2.1 Platform Acceleration Measurements

Accelerometers mounted orthogonally on an inertially stabilized platform, not located at the vehicle center of gravity, sense externally applied special forces and accelerations due to body rotation. The accelerometer measurement is modeled by

$$\underline{a}_m^{(S)} = {}^{S}C^{P}\,{}^{P}C^{P'}\,{}^{P'}C^{B}\left[\frac{\rho A v_m^2}{2m}\underline{c}_f + \frac{\underline{f}_T^{(B)}}{m} + \frac{\underline{f}_P^{(B)}}{m} + \underline{\omega} \times \underline{\omega} \times (\underline{r}_S^{(B)} - \underline{r}_{cg}^{(B)}) + \dot{\underline{\omega}} \times (\underline{r}_S^{(B)} - \underline{r}_{cg}^{(B)})\right] + \underline{b}_a^{(S)} + \underline{v}_a^{(S)} \qquad (32)$$

where

${}^{S}C^{P}$ = transformation from platform coordinates to sensing coordinates

${}^{P}C^{P'}$ = transformation from misaligned platform coordinates to platform coordinates

${}^{P'}C^{B}$ = transformation from body to misaligned platform coordinates

$\underline{r}_S^{(B)}$ = body coordinates of the platform center

$\underline{b}_a^{(S)}$ = accelerometer bias vector

$\underline{v}_a^{(S)}$ = accelerometer measurement noise vector

3.1.2.2 Platform Attitude Measurements

The inertially stabilized platform for the STS is a four axis IMU with a redundant roll axis [4]. Vehicle body attitudes are generated via quaternions [5]. It is assumed that an equivalent representation

can be made to obtain vehicle attitude by a three rotation sequence of roll, pitch, yaw to transform from inertial to body coordiantes. This approach has been used in reference [6].

The attitude angle measurement model is given by

$$\underline{\theta}_m^{(S)} = \underline{\theta} + \underline{b}_\theta^{(S)} + \underline{v}_\theta^{(S)} \tag{33}$$

where

$\underline{b}_\theta$ = platform misalignment bias vector (used to formulate ${}^{P}C^{P'}$)

$\underline{v}_\theta^{(S)}$ = attitude measurement noise vector.

The transformation matrix used to transform from body to inertial coordinates in terms of the elements of the $\underline{\theta}$ vector is given by

$$I_C B = \begin{bmatrix} \cos\theta\cos\psi & \sin\phi\sin\theta\cos\psi - \cos\phi\sin\psi & \cos\phi\sin\theta\cos\psi + \sin\phi\sin\psi \\ \cos\theta\sin\psi & \sin\phi\sin\theta\sin\psi + \cos\phi\cos\psi & \cos\phi\sin\theta\sin\psi - \sin\phi\cos\psi \\ -\sin\theta & \sin\phi\cos\theta & \cos\phi\cos\theta \end{bmatrix} \tag{34}$$

3.1.2.3 Ground Based Tracking Measurements

Ground based radar tracking devices can provide measurements of range, azimuth and elevation from the radar sight to the vehicle. Azimuth and elevation are established relative to the sight's local level. If

the tracking device is a passive optical tracker (not laser) then only azimuth and elevation measurements are available requiring more than one to establish position information.

Defining x, y, and z as the local east, north and up position of the vehicle relative to the ground based tracking device, the radar measurement equations are given by

$$\rho = (x^2 + y^2 + z^2)^{\frac{1}{2}} + b_\rho + v_\rho \tag{35}$$

$$A = \tan^{-1}(\frac{x}{y}) + b_A + v_A \tag{36}$$

$$E = \tan^{-1}(\frac{z}{\sqrt{x^2 + y^2}}) + b_E + \Delta E + v_E \tag{37}$$

where

b_ρ, b_A, b_E = range, azimuth, elevation biases

ΔE = atmospheric refraction correction

v_ρ, v_A, v_E = range, azimuth, elevation measurement noise.

The position vector of the vehicle relative to the tracking device is given by

$$\begin{bmatrix} x \\ y \\ z \end{bmatrix} \triangleq \Delta \underline{r}_V^{(LL)} = {}^{LL}C^{ECF} \left[{}^{ECF}C^{ECI}\, \underline{r}^{(I)} - \underline{r}_{RDR}^{(ECF)} \right] \tag{38}$$

where

$^{LL}_{C}{}^{ECF}$ = transformation from earth center fixed to local level

$^{ECF}_{C}{}^{ECI}$ = earth centered inertial to earth centered fixed

$\underline{r}^{(ECF)}_{RDR}$ = position vector of tracking device in ECF coordinates.

The transformation matrix $^{LL}_{C}{}^{ECF}$ is given by

$$^{ECF}_{C}LL = \begin{bmatrix} -\sin\lambda & -\sin L\cos\lambda & \cos L\cos\lambda \\ \cos\lambda & -\sin L\sin\lambda & \cos L\sin\lambda \\ 0 & \cos L & \sin L \end{bmatrix} \tag{39}$$

where L and λ are the geodetic latitude and east longitude of the device. The transformation matrix $^{ECF}_{C}{}^{ECI}$ is given by

$$^{ECF}_{C}{}^{ECI} = \begin{bmatrix} \cos[\omega_E(t - t_{RNP})] & \sin[\omega_E(t - t_{RNP})] & 0 \\ -\sin[\omega_E(t - t_{RNP})] & \cos[\omega_E(t - t_{RNP})] & 0 \\ 0 & 0 & 1 \end{bmatrix} [RNP] \tag{40}$$

where

ω_E = earth rotation rate

t_{RNP} = time tag for RNP matrix

The position vector, $\underline{r}^{(ECF)}_{RDR}$, of the tracking device is given by

$$\underline{r}_{RDR}^{(ECF)} = \begin{bmatrix} \left(\dfrac{R_E}{\sqrt{\cos^2 L + (1-e)^2 \sin^2 L}} + h\right) \cos L \cos\lambda \\ \left(\dfrac{R_E}{\sqrt{\cos^2 L + (1-e)^2 \sin^2 L}} + h\right) \cos L \sin\lambda \\ \left(\dfrac{R_E(1-e)^2}{\sqrt{\cos^2 L + (1-e)^2 \sin^2 L}} + h\right) \sin L \end{bmatrix} \qquad (41)$$

where

R_E = equatorial radius of Fisher ellipsoid

e = flattening of Fisher ellipsoid

h = altitude of the device above Fisher ellipsoid

3.2 Linearized System State and Measurement Equations

The vehicle equations of motion are nonlinear functions of their motion variables and are implicit functions of other elements of the system states. The measurement equations involve similar function relationships. The linearizations for the filter/smoother algorithm require partial derivatives with respect to the motion variables, i.e., $\underline{v}^{(B)}$ and θ, and with respect to other elements of the state vector, yielding explicit functional relationships for the elements of interest.

For system state equations the partial derivatives will be presented in section 3.2.1 for the state elements in order of occurrence for the first twelve states. Other partial derivatives for candidate state elements will follow in section 3.3.1. The measurement equation partial derivatives for the first twelve states will be presented in section 3.2.2. Partial derivatives of the measurement equations for other candidate states will be presented in section 3.3.2.

The resulting partial derivatives are imbedded into the linearized system state matrix, $F(\underline{x}(t), t)$, as shown in Figure 3.2-1 . A corresponding linearized measurement matrix, $H(\underline{x}_k)$, is similarly formed with the measurement equations' partial derivatives.

3.2.1 System State Partial Derivatives

Partial derivatives of each of the equations listed in Figure 3.2-1 are developed in their order of occurrence with respect to the order of

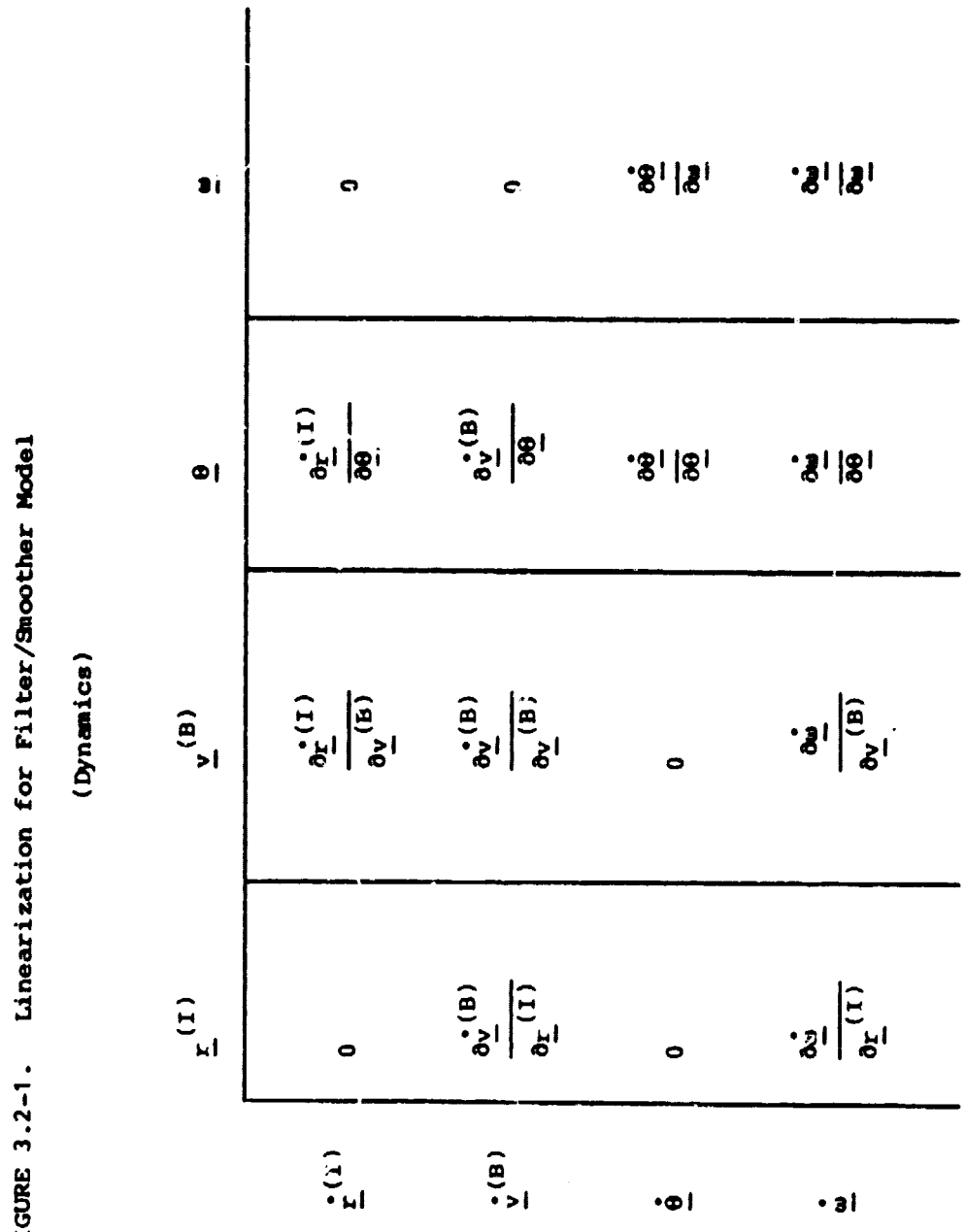

FIGURE 3.2-1. Linearization for Filter/Smoother Model (Dynamics)

the corresponding states. Partial derivatives of thrust terms are presented as though for a single device.

Inertial Position Rate Equation

The first nonzero partial derivative of the $\dot{\underline{r}}^{(I)}$ equation is with respect to $\underline{v}^{(B)}$:

$$\frac{\partial}{\partial \underline{v}^{(B)}} (\dot{\underline{r}}^{(I)}) = {}^{I}C^{B}. \tag{42}$$

The second nonzero partial derivative is with respect to $\underline{\theta}$. This partial derivative results in a third order tensor and occurs frequently in later developments. The generalized form is presented in Appendix A.

Body Velocity Rate Equation

The partial derivative of $\dot{\underline{v}}^{(B)}$ with respect to $\underline{r}^{(I)}$ is given for altitude terms approximately as

$$\frac{\partial}{\partial \underline{r}^{(I)}} = \frac{\partial}{\partial h} \frac{\underline{r}^{(I)^T}}{|\underline{r}^{(I)}|} \tag{43}$$

where

$$\frac{\partial \dot{\underline{v}}^{(B)}}{\partial h} = \frac{Av_m^2}{2m} \frac{\partial \rho}{\partial h} \underline{c}_f + \frac{\rho A v_m}{m} \underline{c}_f \frac{\partial v_m}{\partial h} + \frac{\rho A v_m^2}{2m} \frac{\partial \underline{c}_f}{\partial \alpha} \frac{\partial \alpha}{\partial h} + \frac{\rho A v_m^2}{2m} \frac{\partial \underline{c}_f}{\partial \beta} \frac{\partial \beta}{\partial h}$$

$$+ \frac{1}{m} \left({}^{B}C^{\mathcal{L}} \frac{\partial \underline{f}_T^{(\mathcal{L})}}{\partial p_s} \frac{\partial p_s}{\partial h} + \frac{\partial \underline{f}_p^{(B)}}{\partial h} + \frac{\partial \underline{f}_p^{(B)}}{\partial \alpha} \frac{\partial \alpha}{\partial h} + \frac{\partial \underline{f}_p^{(B)}}{\partial \beta} \frac{\partial \beta}{\partial h} \right) \tag{44}$$

The partial derivatives of $\frac{\partial v_m}{\partial \underline{v}^{(B)}}$, $\frac{\partial \alpha}{\partial \underline{v}^{(B)}}$, $\frac{\partial \beta}{\partial \underline{v}^{(B)}}$, $\frac{\partial \alpha}{\partial h}$, $\frac{\partial \beta}{\partial h}$ and $\frac{\partial v_m}{\partial h}$ occur frequently and are given in Appendix B.

The gravity vector ${}^{B}_{C}I\ \underline{g}^{(I)}(\underline{r}^{(I)})$ partial derivative with respect to $\underline{r}^{(I)}$ is

$$ {}^{B}_{C}I\ \frac{\partial \underline{g}^{(I)}(\underline{r}^{(I)})}{\partial \underline{r}^{(I)}} = {}^{B}_{C}I\ \frac{\mu}{|\underline{r}^{(I)}|^3} \begin{bmatrix} 3\frac{r_1^2}{|\underline{r}|^2} - 1 & 3\frac{r_1 r_2}{|\underline{r}|^2} & 3\frac{r_1 r_2}{|\underline{r}|^2} \\ 3\frac{r_1 r_2}{|\underline{r}|^2} & 3\frac{r_2^2}{|\underline{r}|^2} - 1 & 3\frac{r_2 r_3}{|\underline{r}|^2} \\ 3\frac{r_1 r_3}{|\underline{r}|^2} & 3\frac{r_2 r_3}{|\underline{r}|^2} & 3\frac{r_3^2}{|\underline{r}|^2} - 1 \end{bmatrix} \qquad (45) $$

where

μ = gravitational constant.

The partial derivative, $\frac{\partial \dot{\underline{v}}^{(B)}}{\partial \underline{r}^{(I)}}$, is the sum of the matricies in equations 43 and 45.

The partial derivative of $\dot{\underline{v}}^{(B)}$ with respect to $\underline{v}^{(B)}$ is given by

$$ \frac{\partial \dot{\underline{v}}^{(B)}}{\partial \underline{v}^{(B)}} = \frac{\rho A v_m}{m} \underline{c}_f \frac{\partial v_m}{\partial \underline{v}^{(B)}} + \frac{\rho A v_m^2}{2m} \frac{\partial \underline{c}_f}{\partial \alpha} \frac{\partial \alpha}{\partial \underline{v}^{(B)}} + \frac{\rho A v_m^2}{2m} \frac{\partial \underline{c}_f}{\partial \beta} \frac{\partial \beta}{\partial \underline{v}^{(B)}} $$

$$ + \frac{1}{m} \left[\frac{\partial \underline{f}_p}{\partial \alpha} \frac{\partial \alpha}{\partial \underline{v}^{(B)}} + \frac{\partial \underline{f}_p}{\partial \beta} \frac{\partial \beta}{\partial \underline{v}^{(B)}} \right] - \{\underline{\omega}\} \qquad (46) $$

where

$\{\underline{\omega}\}$ = skew symmetric matrix made from the elements of the vector $\underline{\omega}$ and equivalent to the cross product operator $\underline{\omega} \times (\ )$.

The partial derivative of $\dot{\underline{v}}^{(B)}$ with respect to $\underline{\theta}$ is

$$\frac{\partial \dot{\underline{v}}^{(B)}}{\partial \underline{\theta}} = \frac{\rho A v_m}{m} \underline{c}_f \frac{\partial v_m}{\partial \underline{v}_r} \frac{\partial \underline{v}_r}{\partial \underline{\theta}} + \frac{\rho A v_m^2}{2m} \frac{\partial \underline{c}_f}{\partial \alpha} \frac{\partial \alpha}{\partial \underline{v}_r} \frac{\partial \underline{v}_r}{\partial \underline{\theta}}$$

$$+ \frac{\rho A v_m^2}{2m} \frac{\partial \underline{c}_f}{\partial \beta} \frac{\partial \beta}{\partial \underline{v}_r} \frac{\partial \underline{v}_r}{\partial \underline{\theta}} + \frac{\partial}{\partial \underline{\theta}} [{}^{B}C^{I}\, \underline{g}^{(I)}(\underline{r}^{(I)})]$$

$$+ \frac{1}{m} [\frac{\partial \underline{f}_p^{(B)}}{\partial \alpha} \frac{\partial \alpha}{\partial \underline{v}_r} \frac{\partial \underline{v}_r}{\partial \underline{\theta}} + \frac{\partial \underline{f}_p^{(B)}}{\partial \beta} \frac{\partial \beta}{\partial \underline{v}_r} \frac{\partial \underline{v}_r}{\partial \underline{\theta}}]. \qquad (47)$$

The partial derivatives of $\frac{\partial}{\partial \underline{v}_r}$ are given in Appendix B and the partial derivative $\frac{\partial \underline{v}_r}{\partial \underline{\theta}}$ is given in Appendix A. The last partial derivative is given in Appendix C.

The partial derivative of $\dot{\underline{v}}^{(B)}$ with respect to $\underline{\omega}$ is

$$\frac{\partial \dot{\underline{v}}^{(B)}}{\partial \underline{\omega}} = \frac{\rho A v_m^2}{2m} \frac{\partial \underline{c}_f}{\partial \underline{\omega}} + \{\underline{v}^{(B)}\} \qquad (48)$$

Euler Angle Rate Equation

The Euler angle rate equation is a function of both the Euler angles and the inertial rates. The linearization will yield the two associated matricies.

First with respect to the vector $\underline{\theta}$, the following matrix results

$$\frac{\partial \dot{\underline{\theta}}}{\partial \underline{\theta}} = \begin{bmatrix} q\cos\varphi\tan\theta - r\sin\varphi\tan\theta & q\sin\varphi\sec^2\theta + r\cos\varphi\sec^2\theta & 0 \\ -q\sin\varphi - r\cos\varphi & 0 & 0 \\ q\cos\varphi\sec\theta - r\sin\varphi\cos\theta & q\sin\varphi\sec\theta\tan\theta + r\cos\varphi\sec\theta\tan\theta & 0 \end{bmatrix} \quad (49)$$

The partial derivative of $\dot{\underline{\theta}}$ with respect to $\underline{\omega}$ is

$$\frac{\partial \dot{\underline{\theta}}}{\partial \underline{\omega}} = \begin{bmatrix} 1 & \sin\varphi\tan\theta & \cos\varphi\tan\theta \\ 0 & \cos\varphi & -\sin\varphi \\ 0 & \sin\varphi\sec\theta & \cos\varphi\sec\theta \end{bmatrix} \quad (50)$$

Inertial Angular Acceleration Equation

The first partial derivative of this equation is with respect to the vector $\underline{r}^{(I)}$. Using the approximation indicated in equation 43, this partial derivative is

$$\frac{\partial \dot{\underline{\omega}}}{\partial \underline{r}^{(I)}} = [I]^{-1} \left\{ \frac{Ad v_m^2}{2} \frac{\partial \rho}{\partial h} \underline{c}_m + (\rho v_m Ad \underline{c}_m + (\underline{r}_A^{(B)} - \underline{r}_{cg}^{(B)}) \times \rho v_m A \underline{c}_f) \frac{\partial v_m}{\partial h} \right.$$

$$+ \left(\frac{\rho v_m^2 Ad}{2} \frac{\partial \underline{c}_m}{\partial \alpha} + (\underline{r}_A^{(B)} - \underline{r}_{cg}^{(B)}) \times \frac{\rho v_m^2 A}{2} \frac{\partial \underline{c}_f}{\partial \alpha} \right) \frac{\partial \alpha}{\partial h} \qquad (51)$$

$$+ \left(\frac{\rho v_m^2 Ad}{2} \frac{\partial \underline{c}_m}{\partial \beta} + (\underline{r}_A^{(B)} - \underline{r}_{cg}^{(B)}) \times \frac{\rho v_m^2 A}{2} \frac{\partial \underline{c}_f}{\partial \beta} \right) \frac{\partial \beta}{\partial h}$$

$$\left. + \left((\underline{r}_T^{(B)} - \underline{r}_{cg}^{(B)}) \times {}^{B}C^{\mathcal{L}} \frac{\partial \underline{f}_T^{(\mathcal{L})}}{\partial p_s} \frac{\partial p_s}{\partial h} + \frac{\partial \underline{T}_p}{\partial h} + \frac{\partial \underline{T}_p}{\partial \alpha} \frac{\partial \alpha}{\partial h} + \frac{\partial \underline{T}_p}{\partial \beta} \frac{\partial \beta}{\partial h} \right) \right\} \frac{\underline{r}^{(I)^T}}{|\underline{r}^{(I)}|}$$

Next, with respect to the vector $\underline{v}^{(B)}$, the partial derivative is

$$\frac{\partial \dot{\underline{\omega}}}{\partial \underline{v}^{(B)}} = [I]^{-1} \left\{ (\rho v_m Ad \, \underline{c}_m + (\underline{r}_A^{(B)} - \underline{r}_{cg}^{(B)}) \times \rho v_m A \, \underline{c}_f) \frac{\partial v_m}{\partial \underline{v}^{(B)}} \right.$$

$$+ \left(\frac{\rho v_m^2 Ad}{2} \frac{\partial \underline{c}_m}{\partial \alpha} + (\underline{r}_A^{(B)} - \underline{r}_{cg}^{(B)}) \times \frac{\rho v_m^2 A}{2} \frac{\partial \underline{c}_f}{\partial \alpha} \right) \frac{\partial \alpha}{\partial \underline{v}^{(B)}} \qquad (52)$$

$$+ \left(\frac{\rho v_m^2 Ad}{2} \frac{\partial \underline{c}_m}{\partial \beta} + (\underline{r}_A^{(B)} - \underline{r}_{cg}^{(B)}) \times \frac{\rho v_m^2 A}{2} \frac{\partial \underline{c}_f}{\partial \beta} \right) \frac{\partial \beta}{\partial \underline{v}^{(B)}}$$

$$\left. + \frac{\partial \underline{T}_p}{\partial \alpha} \frac{\partial \alpha}{\partial \underline{v}^{(B)}} + \frac{\partial \underline{T}_p}{\partial \beta} \frac{\partial \beta}{\partial \underline{v}^{(B)}} \right\} .$$

The partial derivative with respect to the vector $\underline{\theta}$ is

$$\frac{\partial \dot{\underline{\omega}}}{\partial \underline{\theta}} = [I]^{-1} \{(\rho v_m Ad\ \underline{c}_m + (\underline{r}_A^{(B)} - \underline{r}_{cg}^{(B)}) \times \rho v_m A\ \underline{c}_f) \frac{\partial v_m}{\partial \underline{\theta}}$$

$$+ (\frac{\rho v_m^2 Ad}{2} \frac{\partial \underline{c}_m}{\partial \alpha} + (\underline{r}_A^{(B)} - \underline{r}_{cg}^{(B)}) \times \frac{\rho v_m^2 A}{2} \frac{\partial \underline{c}_f}{\partial \alpha}) \frac{\partial \alpha}{\partial \underline{\theta}} \qquad (53)$$

$$+ (\frac{\rho v_m^2 Ad}{2} \frac{\partial \underline{c}_m}{\partial \beta} + (\underline{r}_A^{(B)} - \underline{r}_{cg}^{(B)}) \times \frac{\rho v_m^2 A}{2} \frac{\partial \underline{c}_f}{\partial \beta}) \frac{\partial \beta}{\partial \underline{\theta}}$$

$$+ \frac{\partial \underline{T}_p}{\partial \alpha} \frac{\partial \alpha}{\partial \underline{\theta}} + \frac{\partial \underline{T}_p}{\partial \beta} \frac{\partial \beta}{\partial \underline{\theta}} \}.$$

The final partial derivative for the first twelve states is with respect to the vector $\underline{\omega}$. This operation yields

$$\frac{\partial \dot{\underline{\omega}}}{\partial \underline{\omega}} = [I]^{-1} \{\frac{\rho Adv_m^2}{2} \frac{\partial \underline{c}_m}{\partial \underline{\omega}} + \{\underline{r}_A^{(B)} - \underline{r}_{cg}^{(B)}\} \frac{\rho Av_m^2}{2} \frac{\partial \underline{c}_f}{\partial \underline{\omega}}$$

$$+ \{I\underline{\omega}\} - \{\underline{\omega}\} I\} \qquad (54)$$

3.2.2 Measurement Partial Derivatives

The measurements assumed to be available, as discussed earlier, include ground based radar tracking, inertially stabilized platform attitudes relative to the vehicle body, and stabilized platform mounted 3 axis orthogonal accelerations. As with the state dynamics matrix, the measurement equations are linearized about the best state estimates.

Radar Track Measurement Equation

Referring to the radar track measurement equations, the required partial derivatives are

$$\frac{\partial \rho}{\partial \underline{r}^{(I)}} = \frac{\partial \rho}{\partial \Delta \underline{r}_v^{(LL)}} \frac{\partial \Delta \underline{r}_v^{(LL)}}{\partial \underline{r}^{(I)}} \tag{55}$$

$$\frac{\partial A}{\partial \underline{r}^{(I)}} = \frac{\partial A}{\partial \Delta \underline{r}_v^{(LL)}} \frac{\partial \Delta \underline{r}_v^{(LL)}}{\partial \underline{r}^{(I)}} \tag{56}$$

$$\frac{\partial E}{\partial \underline{r}^{(I)}} = \frac{\partial E}{\partial \Delta \underline{r}_v^{(LL)}} \frac{\partial \Delta \underline{r}_v^{(LL)}}{\partial \underline{r}^{(I)}} \,. \tag{57}$$

The last partial derivative in each of these equations, $\frac{\partial \Delta \underline{r}_v^{(LL)}}{\partial \underline{r}^{(I)}}$, is

$$\frac{\partial \Delta \underline{r}_v^{(LL)}}{\partial \underline{r}^{(I)}} = {}^{LL}C^{ECF}\, {}^{ECF}C^{ECI} \,. \tag{58}$$

The rest of the required partial derivatives are

$$\frac{\partial \rho}{\partial \Delta \underline{r}_v^{(LL)}} = \Delta \underline{r}_v^{(LL)^T} / |\Delta \underline{r}_v| \tag{59}$$

$$\frac{\partial A}{\partial \Delta \underline{r}_v^{(LL)}} = \left[\frac{y}{x^2 + y^2}, \quad \frac{-x}{x^2 + y^2}, \quad 0\right] \tag{60}$$

$$\frac{\partial E}{\partial \Delta \underline{r}_v^{(LL)}} = \left[\frac{-xz}{\rho^2 \sqrt{x^2 + y^2}}, \quad \frac{-yz}{\rho^2 \sqrt{x^2 + y^2}}, \quad \frac{\sqrt{x^2 + y^2}}{\rho^2}\right] \tag{61}$$

Inertially Stabilized Platform Attitude Equation

The inertial platform is assumed to provide attitude angle measurements of the true attitude plus an attitude bias plus measurment noise. The partial derivative of the measured attitudes with respect to the vector $\underline{\theta}$ yields an identity matrix.

Accelerometer Measurement Equation

The accelerometer senses specific body forces excluding gravity along the sensing axes. With reference to the accelerometer equation, the partial derivative with respect to $\underline{r}^{(I)}$ is

$$\frac{\partial \underline{a}_m^{(S)}}{\partial \underline{r}^{(I)}} = {}^{S}C^{B}\Big[\frac{\rho A v_m^2}{2m}\frac{\partial \rho}{\partial h}\underline{c}_f + \frac{\rho A v_m}{m}\underline{c}_f\frac{\partial v_m}{\partial h}$$

$$+ \frac{\rho A v_m^2}{2m}\frac{\partial \underline{c}_f}{\partial \alpha}\frac{\partial \alpha}{\partial h} + \frac{\rho A v_m^2}{2m}\frac{\partial \underline{c}_f}{\partial \beta}\frac{\partial \beta}{\partial h} \tag{62}$$

$$+ \frac{1}{m}\Big({}^{B}C^{\mathcal{L}}\frac{\partial \underline{f}_T^{(\mathcal{L})}}{\partial p_s}\frac{\partial p_s}{\partial h} + \frac{\partial \underline{f}_P^{(B)}}{\partial \alpha}\frac{\partial \alpha}{\partial h} + \frac{\partial \underline{f}_P^{(B)}}{\partial \beta}\frac{\partial \beta}{\partial h}\Big)\Big]\frac{\underline{r}^{(I)^T}}{|\underline{r}^{(I)}|}$$

The partial derivative with respect to $\underline{v}^{(B)}$ yields

$$\frac{\partial \underline{a}_m^{(S)}}{\partial \underline{v}^{(B)}} = {}^{S}C^{B}\Big[\frac{\rho A v_m}{m}\underline{c}_f\frac{\partial v_m}{\partial \underline{v}^{(B)}} + \frac{\rho A v_m^2}{2m}\frac{\partial \underline{c}_f}{\partial \alpha}\frac{\partial \alpha}{\partial \underline{v}^{(B)}} + \frac{\rho A v_m^2}{2m}\frac{\partial \underline{c}_f}{\partial \beta}\frac{\partial \beta}{\partial \underline{v}^{(B)}}$$

$$+ \frac{1}{m}\Big[\frac{\partial \underline{f}_P}{\partial \alpha}\frac{\partial \alpha}{\partial \underline{v}^{(B)}} + \frac{\partial \underline{f}_P}{\partial \beta}\frac{\partial \beta}{\partial \underline{v}^{(B)}}\Big] \tag{63}$$

For the partial derivative of the accelerometer with respect to the vector $\underline{\theta}$, the measurement equation is temporarily rewritten as

$$\underline{a}_m^{(S)} = {}^{S}C^{P'}\ {}^{P'}C^{B}\ \underline{s}^{(B)} + \underline{b}_a^{(S)} + \underline{v}_a^{(S)} \tag{64}$$

where the vector $\underline{s}^{(B)}$ represents the sum of the aerodynamic, thrust, plume and rotational coupling terms. The matrix ${}^{P'}C^{B}$ is the same matrix as ${}^{I}C^{B}$. The required partial derivative results from

$$\frac{\partial \underline{a}_m^{(S)}}{\partial \underline{\theta}} = {}^{S_C}P' \quad \frac{\partial}{\partial \underline{\theta}} \quad {}^{I_C}B \; \underline{s}^{(B)} . \tag{65}$$

The partial derivative on the right hand side is developed in Appendix A with the vector $\underline{s}^{(B)}$ representing the sum of the terms indicated above.

The final partial derivative for the accelerometer measurement is with respect to the body rotation vector $\underline{\omega}$. Defining

$$\Delta \underline{r}_s \triangleq \begin{bmatrix} \Delta r_{1_s} \\ \Delta r_{2_s} \\ \Delta r_{3_s} \end{bmatrix} = (\underline{r}_s^{(B)} - \underline{r}_{cg}^{(B)}) \tag{66}$$

and denoting ω_i as the i^{th} element of the vector $\underline{\omega}$, the resulting matrix is

$$\frac{\partial \underline{a}_m}{\partial \underline{\omega}} = {}^{S_C}B \begin{bmatrix} \omega_2\Delta r_2 + \omega_3\Delta r_3 & \omega_1\Delta r_2 - 2\omega_2\Delta r_1 & \omega_1\Delta r_3 - 2\omega_3\Delta r_1 \\ \omega_2\Delta r_1 - 2\omega_1\Delta r_2 & \omega_1\Delta r_1 + \omega_3\Delta r_3 & \omega_2\Delta r_3 - 2\omega_3\Delta r_2 \\ \omega_3\Delta r_1 - 2\omega_1\Delta r_3 & \omega_3\Delta r_2 - 2\omega_2\Delta r_3 & \omega_1\Delta r_1 + \omega_2\Delta r_2 \end{bmatrix} \tag{67}$$

3.2.3 Additional Parameter Partial Derivatives

The mathematical developments are presented in this section for the partial derivatives of the system and measurement equations to allow for additional candidate parameters to be included in the estimation algorithms. These parameters include center-of-gravity, $\underline{r}_{cg}$, moments of inertia, I, wind velocity, $\underline{v}_w$, and inertial platform tilt errors. Aerodynamic and plume parameter partial derivatives are also presented.

The computer program is being structured to permit these parameters to be easily incorporated without significant impact on the program code.

3.2.3.1 Center-of-Gravity

From equation 23, the partial derivative of angular acceleration with respect to $\underline{r}_{cg}$ is

$$\frac{\partial \dot{\underline{\omega}}}{\partial \underline{r}_{cg}} = [I]^{-1} \left[\frac{\rho A v_m^2}{2} \left\{ \underline{c}_f \right\} + \sum_{i=1}^{n} \left\{ {}^{B}C_i^{\mathcal{L}} \begin{bmatrix} f_{T_i}^{\mathcal{L}} \\ 0 \\ 0 \end{bmatrix} \right\} \right] \tag{68}$$

From equation 32, the partial derivative of the measured acceleration with respect to $\underline{r}_{cg}$ is

$$\frac{\partial \underline{m}}{\partial \underline{r}_{cg}} = -{}^{S}C^{B} \left\{ \underline{\omega} \times \underline{\omega} \right\} \tag{69}$$

3.2.3.2 Moments of Inertia

The moments-of-inertia are grouped into "principal" terms, $\underline{i}_p$, and cross product terms, $\underline{i}_{cp}$. From equation 24, these vectors are defined as

$$\underline{i}_p = \begin{bmatrix} I_x \\ I_y \\ I_z \end{bmatrix} \tag{70}$$

and

$$\underline{i}_{cp} = \begin{bmatrix} I_{xy} \\ I_{zx} \\ I_{yz} \end{bmatrix} \tag{71}$$

With these definitions, equation 23 is rewritten as

$$\dot{\underline{\omega}} = [I]^{-1} \left[\Sigma \underline{T} - \{\underline{\omega}\} \left\{ \begin{bmatrix} \omega_1 & 0 & 0 \\ 0 & \omega_2 & 0 \\ 0 & 0 & \omega_3 \end{bmatrix} \underline{i}_p + \begin{bmatrix} -\omega_2 & -\omega_3 & 0 \\ -\omega_1 & 0 & -\omega_3 \\ 0 & -\omega_1 & -\omega_2 \end{bmatrix} \underline{i}_{cp} \right\} \right] \tag{72}$$

where $\Sigma\underline{T}$ represents the sum of the nonrotational torques in equation 23. Defining an intermediate vector $\underline{a}$ as

$$\underline{a} = \Sigma\underline{T} - \underline{\omega} \times (I\underline{\omega}) \tag{73}$$

the partial derivatives of the angular acceleration with respect to $\underline{i}_p$ and $\underline{i}_{cp}$ are

$$\frac{\partial \dot{\underline{\omega}}}{\partial \underline{i}_p} = \frac{\partial}{\partial \underline{i}_p}\left(I^{-1}\,\underline{a}\right)\Big|_{\underline{a}\text{-fixed}} - (I)^{-1}\begin{bmatrix} 0 & -\omega_2\omega_3 & \omega_2\omega_3 \\ \omega_1\omega_3 & 0 & -\omega_1\omega_3 \\ -\omega_1\omega_2 & \omega_1\omega_2 & 0 \end{bmatrix} \tag{74}$$

and

$$\frac{\partial \dot{\underline{\omega}}}{\partial \underline{i}_{cp}} = \frac{\partial}{\partial \underline{i}_{cp}}\left(I^{-1}\,\underline{a}\right)\Big|_{\underline{a}\text{-fixed}} - [I]^{-1}\begin{bmatrix} \omega_1\omega_2 & -\omega_1\omega_2 & \omega_3^2 - \omega_2^2 \\ -\omega_2\omega_3 & \omega^2 - \omega_3^2 & \omega_1\omega_2 \\ \omega_2^2 - \omega_1^2 & \omega_2\omega_3 & -\omega_1\omega_3 \end{bmatrix} \tag{75}$$

where

$$\frac{\partial}{\partial \underline{i}_p}(I^{-1}\,\underline{a}) = \frac{1}{\Delta}\begin{bmatrix} 0 & I_z a_1 + I_{zx} a_3 & I_y a_1 + I_{xy} a_2 \\ I_z a_2 + I_{yz} a_3 & 0 & I_x a_2 + I_{xy} a_1 \\ I_y a_3 + I_{yz} a_2 & I_x a_3 + I_{zx} a_1 & 0 \end{bmatrix} \tag{76}$$

$$- [I]^{-1}\,\frac{1}{\Delta}\begin{bmatrix} (I_y I_z - I_{yz}^2)a_1 & (I_x I_z - I_{zx}^2)a_1 & (I_x I_y - I_{xy}^2)a_1 \\ (\quad " \quad)a_2 & (\quad " \quad)a_2 & (\quad " \quad)a_2 \\ (\quad " \quad)a_3 & (\quad " \quad)a_3 & (\quad " \quad)a_3 \end{bmatrix}$$

and

$$\frac{\partial}{\partial \underline{i}_{cp}}(I^{-1}\,a) =$$

(77)

$$= \frac{1}{\Delta}\begin{bmatrix} I_z a_2 + I_{yz} a_3 & I_y a_3 + I_{yz} a_2 & -2I_{yz} a_1 + I_{zx} a_2 + I_{xy} a_3 \\ I_z a_1 + I_{zx} a_3 & I_{yz} a_1 - 2I_{zx} a_2 + I_{xy} a_3 & I_x a_3 + I_{zx} a_1 \\ I_{yz} a_1 + I_{zx} a_2 - 2I_{xy} a_3 & I_y a_1 + I_{xy} a_2 & I_x a_2 + I_{xy} a_1 \end{bmatrix}$$

$$- [I]^{-1} \frac{1}{\Delta} \begin{bmatrix} -2(I_z I_{xy} + I_{zx} I_{yz})a_1 & -2(I_y I_{zx} + I_{xy} I_{yz})a_1 & -2(I_x I_{yz} + I_{xy} I_{xz})a_1 \\ -2(\quad " \quad)a_2 & -2(\quad " \quad)a_2 & -2(\quad " \quad)a_2 \\ -2(\quad " \quad)a_3 & -2(\quad " \quad)a_3 & -2(\quad) \quad)a_3 \end{bmatrix}$$

and

$$\Delta = I_x I_y I_z - I_{xy} I_{yz} I_{zx} - I_{zx} I_{xy} I_{yz} - I_y I_{zx}^2 - I_z I_{xy}^2 - I_x I_{yz}^2 \qquad (78)$$

3.2.3.3 Wind Velocity

From equations 20 and 25, the partial derivative of the vehicle acceleration with respect to $\underline{v}_w$ is

$$\frac{\partial \dot{\underline{v}}^{(B)}}{\partial \underline{v}_w} = \frac{\rho A}{2m} \underline{c}_f \frac{\partial v_m^2}{\partial \underline{v}_w} + \frac{\rho A v_m^2}{2m} \frac{\partial \underline{c}_f}{\partial \alpha} \frac{\partial \alpha}{\partial \underline{v}_w} + \frac{\rho A v_m^2}{2m} \frac{\partial \underline{c}_f}{\partial \beta} \frac{\partial \beta}{\partial \underline{v}_w} . \qquad (79)$$

The first of the partial derivatives in equation 79 can be obtained from the following equation

$$v_m^2 = \underline{v}_r^T \underline{v}_r = \underline{v}^{(B)^T} \underline{v}^{(B)} - 2\underline{v}^{(B)^T} B_C \underline{v}_w + \underline{v}_w^T C^B B_C \underline{v}_w \qquad (80)$$

From equation 80, the following is obtained

$$\frac{\partial v_m^2}{\partial \underline{v}_w} = - 2 \underline{v}_r^T B_C. \qquad (81)$$

Denoting the elements of the matrix ${}^{B}C$ as c_{11}, c_{12}, etc., the following equations are obtained for the partial derivatives of α and β with respect to $\underline{v}_w$;

$$\frac{\partial \alpha}{\partial \underline{v}_w} = \frac{-1}{v_{r_1}^2 + v_{r_3}^2} \begin{bmatrix} (v_{r_1} c_{31} - v_{r_3} c_{11}) \\ (v_{r_1} c_{32} - v_{r_3} c_{12}) \\ (v_{r_1} c_{33} - v_{r_3} c_{13}) \end{bmatrix}^T \tag{82}$$

and

$$\frac{\partial \beta}{\partial \underline{v}_w} = \frac{-1}{v_m \sqrt{v_{r_2}^2 + v_{r_3}^2}} \begin{bmatrix} v_m c_{21} - \frac{v_{r_2}}{v_m} (v_{r_1} c_{11} + v_{r_2} c_{21} + v_{r_3} c_{31}) \\ v_m c_{22} - \frac{v_{r_2}}{v_m} (v_{r_1} c_{12} + v_{r_2} c_{22} + v_{r_3} c_{32}) \\ v_m c_{23} - \frac{v_{r_2}}{v_m} (v_{r_1} c_{13} + v_{r_2} c_{23} + v_{r_3} c_{33}) \end{bmatrix}^T \tag{83}$$

3.2.3.4 Inertial Platform Tilt

Temporarily rewriting equation (32) as

$$\underline{a}_m^{(S)} = {}^{S}C^{P}(I + \underline{\delta\theta} \times) \underline{s} \tag{84}$$

where

$\underline{\delta\theta}$ = vector whose elements are the axes misalignments

$\underline{s}$ = sum of the bracketed terms in equation 32 multiplied by ${}^{P'}C^{B}$.

The following partial derivative of the measured acceleration with respect to $\underline{\delta\theta}$ is obtained

$$\frac{\partial \underline{a}_m^{(S)}}{\partial \underline{\delta\theta}} = {}^{S}C^{P} \, \underline{\tilde{s}}, \tag{85}$$

3.2.3.5 Aerodynamic and Plume Parameters

A linear model for the aerodynamic and plume characteristics is used. This model is expanded as

$$\underline{c}_f = \underline{c}_{fo} + \underline{c}_{f\alpha}\,\alpha + \underline{c}_{f\beta}\,\beta + \ldots \tag{86}$$

and

$$\underline{c}_m = \underline{c}_{mo} + \underline{c}_{m\alpha}\,\alpha + \underline{c}_{m\beta}\,\beta + \ldots \tag{87}$$

$$\underline{f}_p = \underline{f}_p + \underline{f}_{p\alpha}\,\alpha + \underline{f}_{p\beta}\,\beta + \ldots \tag{88}$$

where additional terms to represent rates, cross couplings, and controls can be included.

The basic approach of estcblishing the partial derivatives will be illustrated for a couple of terms, $\underline{c}_{f\alpha}$ and $\underline{c}_{m\alpha}$. Using these example

illustrations, the rest of the candidate parameters can be similarly obtained. From equation 20, the following partial derivative is obtained

$$\frac{\partial \dot{\underline{v}}^{(B)}}{\partial \underline{c}_{f_\alpha}} = \frac{\partial \underline{v}^{(B)}}{\partial \underline{c}_f} \frac{\partial \underline{c}_f}{\partial \underline{c}_{f_\alpha}} = \frac{\rho A v_m^2}{2m} \alpha[U] \tag{89}$$

where

[U] = unit 3 x 3 matrix with one's (1) on the diagonal and zeros off the diagonal

From equation 23, the partial derivative of angular acceleration with respect to $\underline{c}_{m_\alpha}$ is

$$\frac{\partial \dot{\underline{\omega}}}{\partial \underline{c}_{m_\alpha}} = \frac{\partial \dot{\underline{\omega}}}{\partial \underline{c}_m} \frac{\partial \underline{c}_m}{\partial \underline{c}_{m_\alpha}} = [I]^{-1} \frac{\rho A v_m^2}{2} \alpha[U]. \tag{90}$$

The corresponding partial derivative with respect to $\underline{c}_{f_\alpha}$ is

$$\frac{\partial \dot{\underline{\omega}}}{\partial \underline{c}_{f_\alpha}} = \frac{\partial \dot{\underline{\omega}}}{\partial \underline{c}_f} \frac{\partial \underline{c}_f}{\partial \underline{c}_{f_\alpha}} = [I]^{-1} \frac{\rho A v_m^2}{2} \left\{ \underline{r}_A^{(B)} - \underline{r}_{cg}^{(B)} \right\} \alpha[U]. \tag{91}$$

The static aerodynamic coefficient model has been obtained by a multiple regression analysis of the current aerodynamic tabular data. This model is presented in Appendix D with the associated regression coefficients.

3.3 Propulsion Parameter States and Measurements

A candidate approach for incorporating the NASA propulsion model's capabilities has been identified. This approach utilizes nominal predicted values of thrust, pressure, propellant and pressurant mass flow rates, and utilizes sensitivities or partial derivatives of these variables with respect to the independent parameters selected for estimation by the algorithm.

The approach is to include deviations from nominal values of measured chamber pressure, power level, propellant and pressurant mass flow rates as states. The models assumed for these deviations are time correlated random processes. Then as states, partial derivatives of the first twelve states with respect to these variables will be required.

For the SSME and SRB, this modeling approach is discussed in the following. Additionally, the necessary partial derivatives of the first twelve state variables with resepct to the additional states are presented.

3.3.1 SSME Propulsion Parameter Model

For the SSME, the total actual values of vacuum thrust and oxidizer mass flow rates are modeled by

$$f_T = f_{T_{nom}} + \Delta f_T \tag{92}$$

and

$$\dot{m}_{O_2} = \dot{m}_{O_{2_{nom}}} + \Delta\dot{m}_{O_2}. \tag{93}$$

The measurements of fuel mass flow rate, pressurant mass flow rates and power level are modeled as

$$\dot{m}_{H_2} = \dot{m}_{H_{2_{nom}}} + \Delta\dot{m}_{H_2} + b_{\dot{m}_{H_2}} + s_{\dot{m}_{H_2}} \tag{94}$$

$$\dot{m}_{H_{2_p}} = \dot{m}_{H_{2_{p_{nom}}}} + \Delta\dot{m}_{H_{2_p}} + b_{\dot{m}_{H_{2_p}}} + s_{\dot{m}_{H_{2_p}}} \tag{95}$$

$$\dot{m}_{O_{2_p}} = \dot{m}_{O_{2_{p_{nom}}}} + \Delta\dot{m}_{O_{2_p}} + b_{\dot{m}_{O_{2_p}}} + s_{\dot{m}_{O_{2_p}}} \tag{96}$$

and

$$PL = PL_{nom} + \Delta PL + b_{PL} + s_{PL}. \tag{97}$$

These measured quantities include measurement noise $s_{(\ )}$ and potential bias states $b_{(\ )}$ modeled as random constants. In these measurements, the Δ'd variables are to be included as states in the estimation algorithm. If the nominal values are zero or unknown, then the Δ'd variables absorb the entire estimate. Where required, the estimate for the variables used in the estimation algorithm is formed using the nominal and the estimate of the deviation, etc. In example, thrust and fuel mass flow rate estimates are formed as

$$\hat{f}_T = f_{T_{nom}} + \hat{\Delta f}_T \tag{98}$$

and

$$\hat{\dot{m}}_{H_2} = \dot{m}_{H_{2_{nom}}} + \hat{\Delta\dot{m}}_{H_2} + \hat{b}_{\dot{m}_{H_2}} . \tag{99}$$

The deviation or Δ'd measurement variables are modeled as time correlated random variables. This permits these variables to vary within a band of frequencies. The typical model is then given as

$$\frac{d}{dt}\Delta(\ ) = -\frac{1}{\tau_{(\ )}}\Delta(\ ) + \frac{1}{\tau_{(\ )}} s_{(\ )} \tag{100}$$

where the parenthesis ( ) would be replaced by the variables, i.e., $\dot{m}_{H_2}$. For the SSME, an additional variable Δc^*_{mult} is modeled as in equation 100 and included as a state variable with the Δ'd measurement variables.

The thrust deviation is expanded as in the following truncated Taylor series as a function of the independent parameters.

$$\Delta f_T = \frac{\partial f_T}{\partial \dot{m}_{H_{2_p}}} \Delta\dot{m}_{H_{2_p}} + \frac{\partial f_T}{\partial \dot{m}_{O_{2_p}}} \Delta\dot{m}_{O_{2_p}} + \frac{\partial f_T}{\partial \Delta c^*} \Delta c^*$$

$$+ \frac{\partial f_T}{\partial PL} \Delta PL + \frac{\partial f_T}{\partial MR} \Delta MR. \tag{101}$$

In the $\underline{\dot{v}}^{(B)}$ and $\underline{\dot{\omega}}$ equations, with equation 101 replacing f_{T_i}, the partial derivatives of f_T with respect to the Δ'd variables are obtained directly from equation 101.

It is desirable to include vehicle mass bias as a state. The SSME's system contribution to the mass deviation is given by

$$\Delta\dot{m}_{SSME's} = \sum_i (\Delta\dot{m}_{H_{2_i}} + \Delta\dot{m}_{O_{2_i}} - \Delta\dot{m}_{H_{2_{p_i}}} - \Delta\dot{m}_{O_{2_{p_i}}}). \tag{102}$$

In equation 101, the Δm_{O_2} contribution to the mass deviation is not available from measurements. As with the thrust deviation, this quantity is formed as

$$\Delta\dot{m}_{O_2} = \frac{\partial\dot{m}_{O_2}}{\partial\dot{m}_{H_{2_p}}} \Delta\dot{m}_{H_{2_p}} + \frac{\partial\dot{m}_{O_2}}{\partial\dot{m}_{O_{2_p}}} \Delta\dot{m}_{O_{2_p}} + \frac{\partial\dot{m}_{O_2}}{\partial\Delta c^*} \Delta c^* + \frac{\partial\dot{m}_{O_2}}{\partial PL} \Delta PL + \frac{\partial\dot{m}_{O_2}}{\partial MR} \Delta MR. \tag{103}$$

which is in terms of other estimated state variables. In equations 101 and 103 the deviation in mixture ratio, ΔMR, is obtained algebraically from

$$\Delta MR = \frac{\dot{m}_{H_{2_{nom}}} - \hat{\dot{m}}_{H_2}}{\frac{\partial\dot{m}_{H_2}}{\partial MR}} \tag{104}$$

The partial derivatives for the SSME above have been incorporated into the estimation algorithm as functions of engine power level.

3.3.2 SRB Propulsion Parameter Model

The approach for the SRB modeling follows closely that used for the SSME. Candidate independent parameters include propellant burn rate exponent, a, and motor efficiency coefficient, c_m. Others can be added using this technique.

The actual value of vacuum thrust is given by equation 92. The only measurement available for the SRB is the total pressure at the forward head end of the motor case and is modeled as

$$P_{O_H} = P_{O_{H_{nom}}} + \Delta P_{O_H} + b_{P_{O_H}} + s_{P_{O_H}} \tag{105}$$

where $b_{(\ )}$ and $s_{(\ )}$ represents a bias and measurement noise respectively.

The independent parameters, Δa and Δc_m, are included in the model as states. The model assumed can be as given by equation 100 or another suitable dynamical process, i.e., random constant.

The thrust deviation is given by the following truncated Taylor series as a function of the candidate independent parameters.

$$\Delta f_T = \frac{\partial f_T}{\partial a}\Delta a + \frac{\partial f_T}{\partial c_m}\Delta c_m + \ldots \tag{106}$$

The partial derivatives for the $\dot{\underline{v}}^{(B)}$ and $\dot{\underline{\omega}}$ equations with respect to the independent parameters are obtained directly from equation 106. The mass deviation equation for the SRB is given as

$$\Delta\dot{m}_{SRB} = \sum_i (\Delta\dot{m})_i \tag{107}$$

where

$$\Delta\dot{m}_i = \frac{\partial \dot{m}}{\partial a} \Delta a + \ldots \tag{108}$$

The head pressure deviation, ΔP_{O_H}, is expanded similarly

$$\Delta P_{O_H} = \frac{\partial P_{O_H}}{\partial a} \Delta a + \ldots \tag{109}$$

A simplified model for the SRB's thrust, head pressure and mass flow rate has been developed that can be directly incorporated within the filter algorithm for estimating burn rate coefficient, nozzle coefficient, mass flow rate, etc. This model, to be described below, uses apriori specified burn area and port volume as a function of burn depth into the propellant grain. From this simplified model analytical partial derivatives required by the estimation algorithm can be obtained.

The thrust is given by

$$f_T = c_m \, c_T \, c^* \, \dot{m}/g \tag{110}$$

where

c_m = nozzle coefficient

c_T = thrust coefficient

c^* = characteristic exhaust velocity

$\dot{m}$ = mass flow rate

g = gravity acceleration

Two of the required partial derivatives with respect to mass flow rate and nozzle coefficient are easily obtained, vis

$$\frac{\delta f_T}{\delta \dot{m}} = c_T c^* c_m \tag{111}$$

and

$$\frac{\delta f_T}{\delta c_m} = c_T c^* \dot{m} \tag{112}$$

The partial derivative with respect to burn rate coefficient is

$$\frac{\delta f_T}{\delta a} = \left[\frac{\delta c_T}{\delta P_O} \frac{\delta P_O}{\delta a} \dot{m} + \frac{\delta \dot{m}}{\delta a} c_T\right] c^* c_m \tag{113}$$

where it has been assumed that c^* is not a function of a. Using the "ideal" expression for c_T [7]

$$c_T = \sqrt{\frac{2\gamma^2}{\gamma-1}\left(\frac{2}{\gamma+1}\right)^{\frac{\gamma+1}{\gamma-1}}\left[1 - \left(\frac{P_e}{P_O}\right)^{\frac{\gamma-1}{\gamma}}\right]} + \frac{P_e - P_a}{A_t}\frac{A_e}{P_O}, \tag{114}$$

where

γ = ratio of specific heats

P_e = motor nozzle exit pressure

P_a = ambient atmospheric pressure at nozzle exit

A_e = motor nozzle exit area

A_t = motor nozzle throat area,

the first partial derivative in equation 113 is

$$\frac{\partial c_T}{\partial P_O} = \frac{1}{2}\sqrt{\frac{\frac{2\gamma^2}{\gamma-1}\left(\frac{2}{\gamma+1}\right)^{\frac{\gamma+1}{\gamma-1}}}{\left[1-\left(\frac{P_e}{P_O}\right)^{\frac{\gamma-1}{\gamma}}\right]}}\left[\left(\frac{\gamma-1}{\gamma}\right)\left(\frac{P_e}{P_O}\right)^{\frac{\gamma-1}{\gamma}}\right]\frac{1}{P_O} - \frac{P_e - P_a}{A_t}\frac{A_e}{P_O^2} \qquad (115)$$

To evaluate the second partial derivative in equation 113, the following equation for pressure [8] is used:

$$P_O = \left(\frac{c^* \rho_p a A_b}{A_t}\right)^{\frac{1}{1-n}} \qquad (116)$$

where

ρ_p = propellant density

A_b = propellant burn area

n = propellant burn rate exponent

The following partial derivative is then obtained

$$\frac{\partial P_O}{\partial a} = \left(\frac{c^* \rho A_b}{g A_t}\right)^{\frac{1}{1-n}} \left(\frac{1}{1-n}\right) a^{\frac{n}{1-n}} \qquad (117)$$

The last partial derivative in equation 113 is obtained from

$$\dot{m} = \rho_p r_b A_b = \rho_p a\left(\frac{c^* \rho a A_b}{g A_t}\right)^{\frac{n}{1-n}} A_b. \qquad (118)$$

The resulting partial derivative is

$$\frac{\partial \dot{m}}{\partial a} = \rho_p \left(\frac{c^* \rho_p a}{g A_t}\right)^{\frac{n}{1-n}} \left(\frac{1}{1-n}\right) A_b^{\frac{1}{1-n}} \qquad (119)$$

To utilize the head pressure measurement and its sensitivity to parameter variations, the following equation [7] is used

$$P_{O_H} = \frac{P_O}{2}\left[1 + \sqrt{1 + 4RT\left(\frac{c r_b \rho_p \ell}{A_p P_O}\right)}\right] \tag{120}$$

where

R = gas constant

T = gas absolute temperature

c = port circumference

A_p = port cross section area

r_b = propellant burn rate

ℓ = distance from motor nozzle to pressure measurement point

This equation assumes a cylindrical port with an approximately constant cross sectional area.

With this assumption $\frac{c\ell}{A_p}$ becomes $\sqrt{4\pi\frac{\ell^3}{V_p}}$. Also recognizing that

$$\frac{\rho_p r_b}{P_O} = \rho_p a P_O^{n-1} = \rho_p a\left(\frac{c^* \rho_p a A_b}{A_t}\right)^{\frac{n-1}{1-n}} = \rho_p a\left(\frac{c^* \rho_p a A_b}{A_t}\right)^{-1} = \frac{A_t}{c^* A_b},$$

then equation (120) can be rewritten as

$$P_{O_H} = \frac{P_O}{2}\left[1 + \sqrt{1 + 16\pi RT \frac{\ell^3}{V_p}\left(\frac{A_t}{c^* A_b}\right)^2}\right].$$

The partial derivatives with respect to burn rate coefficient and mass flow rate are

$$\frac{\partial P_{O_H}}{\partial a} = \frac{1}{2}\left[1 + \sqrt{1 + 16\pi RT \frac{\ell^3}{V_p}\left(\frac{A_t}{c^* A_b}\right)^2}\right] \frac{\partial P_O}{\partial a} \tag{121}$$

and

$$\frac{\partial P_{O_H}}{\partial \dot{m}} = \frac{1}{2}\left\{\left[1 + \frac{1}{\sqrt{1 + 4RT\left(\frac{\dot{m}\ell}{V_p P_O}\right)^2}}\right]\frac{\partial P_O}{\partial \dot{m}} + \frac{4RT\frac{\dot{m}\ell^2}{V^2 P_O}}{\sqrt{1 + 4RT\left(\frac{\dot{m}\ell}{V_p P_O}\right)^2}}\right\} \qquad (122)$$

In equations 121 and 122 a cylindrical port has been assumed in determining the port volume V_p. Equation 122 was obtained from equation 120 by replacing the term $c\, r_b\, \rho_p\, \ell$ by $\dot{m}$. The partial derivative of P_{O_H} with respect to c_m is obviously zero. In using these analytical partial derivatives, the basic performance measures of thrust, mass flow rate, head and nozzle pressures, etc. are matched between this model and the NASA SOBER internal ballistics routine results. The burn area and port volume are adjusted in the simple model to obtain the agreement. Then using the adjusted area and volume as a function of burn depth, the partial derivatives are evalauted.

The inclusion of solid propellant thickness, τ, as a state variable necessitates the development of the partial derivatives of τ with respect to the solid propulsion parameters and the partial derivative of the measurement P_{O_H} with respect to τ. These partial derivatives are given as

$$\frac{\partial \dot{\tau}}{\partial a} = \frac{1}{1-n}\left(\frac{c^* \rho \lambda_b a}{g A_t}\right)^{\frac{n}{1-n}} \qquad (123)$$

and

$$\frac{\partial P_{O_H}}{\partial \tau} = \tfrac{1}{2}\left[\left(1 + 16\pi RT \frac{\ell^3}{V_p}\left(\frac{A_t}{c^* A_b}\right)^2\right)\right] \frac{\partial P_O}{\partial \tau}$$

$$+ \frac{8\pi RT \frac{\ell^3}{V_p} \cdot P_O \frac{\partial}{\partial \tau}\left(\frac{A_t}{c^* A_b}\right)^2}{\sqrt{16\pi RT \frac{\ell^3}{V_p}\left(\frac{A_t}{c^* A_b}\right)^2}} \qquad (124)$$

where

$$\frac{\partial P_O}{\partial \tau} = \left[\frac{\rho a A_b}{A_t}\frac{\partial c^*}{\partial P_O}\frac{\partial P_O}{\partial \tau} + \frac{c^* \rho a}{A_t}\frac{\partial A_b}{\partial \tau} + c^* \rho a A_b \frac{\partial \frac{1}{A_t}}{\partial P_O}\frac{\partial P_O}{\partial \tau}\right]\left(\frac{1}{1-n}\right)\left(\frac{c^* \rho a A_b}{g A_t}\right)^{\frac{n}{1-n}} \qquad (125)$$

Here, the partial derivatives of c^*, A_b, and A_t with respect to τ are evaluated numerically.

Finally, the partial derivative of thrust with respect to τ is given by

$$\frac{\partial f_T}{\partial \tau} = C_T \frac{\partial P_O}{\partial \tau} A_t + C_T P_O \frac{\partial A_t}{\partial P_O}\frac{\partial P_O}{\partial \tau} \qquad (126)$$

3.3.3 Vehicle Mass

The total rate of change of vehicle mass is given by

$$\frac{d}{dt}(m) = \dot{m}_{SSME_{nom}} + \dot{m}_{SRB_{nom}} + \Delta\dot{m}_{SSME} + \Delta\dot{m}_{SRB} + \dot{m}_{NON-CONSUME} \qquad (127)$$

The first two terms in this equation are the apriori assumed nominal values. The third and fourth terms were discussed earlier. The last term should be zero; however it can include a mass bias uncertainty Δm_b.

The equations, state and measurement, in which mass occurs are the $\underline{\dot{v}}^{(B)}$ and $\underline{a}_m$ equations. Assuming equation 123 can be summarized as $\dot{m} + \Delta\dot{m}_b$ then the mass can be written as $m + \Delta m_b$. Replacing this expression for the mass in the two indicated equations yields the following partial derivatives with respect to the Δm_b.

$$\frac{\partial \underline{v}^{(B)}}{\partial \Delta m_b} = -\frac{1}{(m + \Delta m_b)^2}\left(\frac{\rho v_m^2 A}{2}\ \underline{c}_f + \underline{f}_p^{(B)} + {}^{B}C^{\mathcal{L}}\ \underline{f}_{T_i}^{(\mathcal{L})}\right) \qquad (128)$$

and

$$\frac{\partial \underline{a}_m^{(S)}}{\partial \Delta m_b} = -\frac{1}{(m + \Delta m_b)^2}\ {}^{S}C^{B}\left(\frac{\rho v_m^2 A}{2}\ \underline{c}_f + \underline{f}_p^{(B)} + {}^{B}C^{\mathcal{L}}\ \underline{f}_{T_i}^{(\mathcal{L})}\right) \qquad (129)$$

4.0 COMPUTER PROGRAM DESCRIPTIONS

The optimal estimation techniques described in the previous sections have been implemented into two computer programs which reside in NASA's VAX computer. These programs are structured in a highly modular approach facilitating easy modification and additions. The two programs, identified in VAX nomenclature as FILTER.EXE and SMOOTH.EXE, are described below. The linearized state and measurement equations implemented into the programs are shown in Figures 4.0-1 and 4.0-2, with the indicated partial derivatives developed in Section 3.0. A listing of the FORTRAN code for these two programs are provided in Volumn II of this report.

4.1 FILTER Program Description

The interconnection of the major routines for the FILTER program is shown in Figure 4.1-1. The basic flow of the program is a sequential processing of measured data available at discrete time instances and propagating the state estimate vector and error covariance matrix forward to the next time measurements are available.

Between measurements, the state vector, formed in XDVEC, and the error covariance matrix, formed in PDMTRX, are propagated forward (integrated in time) using a Runge-Kutta fourth order numerical integration algorithm RK4FIL. The subroutine GETDAT reads the measurement data from disk file INPUT.DAT. The subroutine MEASUR calls the various routines to update the state estimate based on available measurement data. These routines are: RADAR for radar azimuth, elevation and range data for three radars; ACCEL for three axis accelerometer measurements on the inertially stabilized platform; ATTIT for the attitudes available from the platform; SSME for the

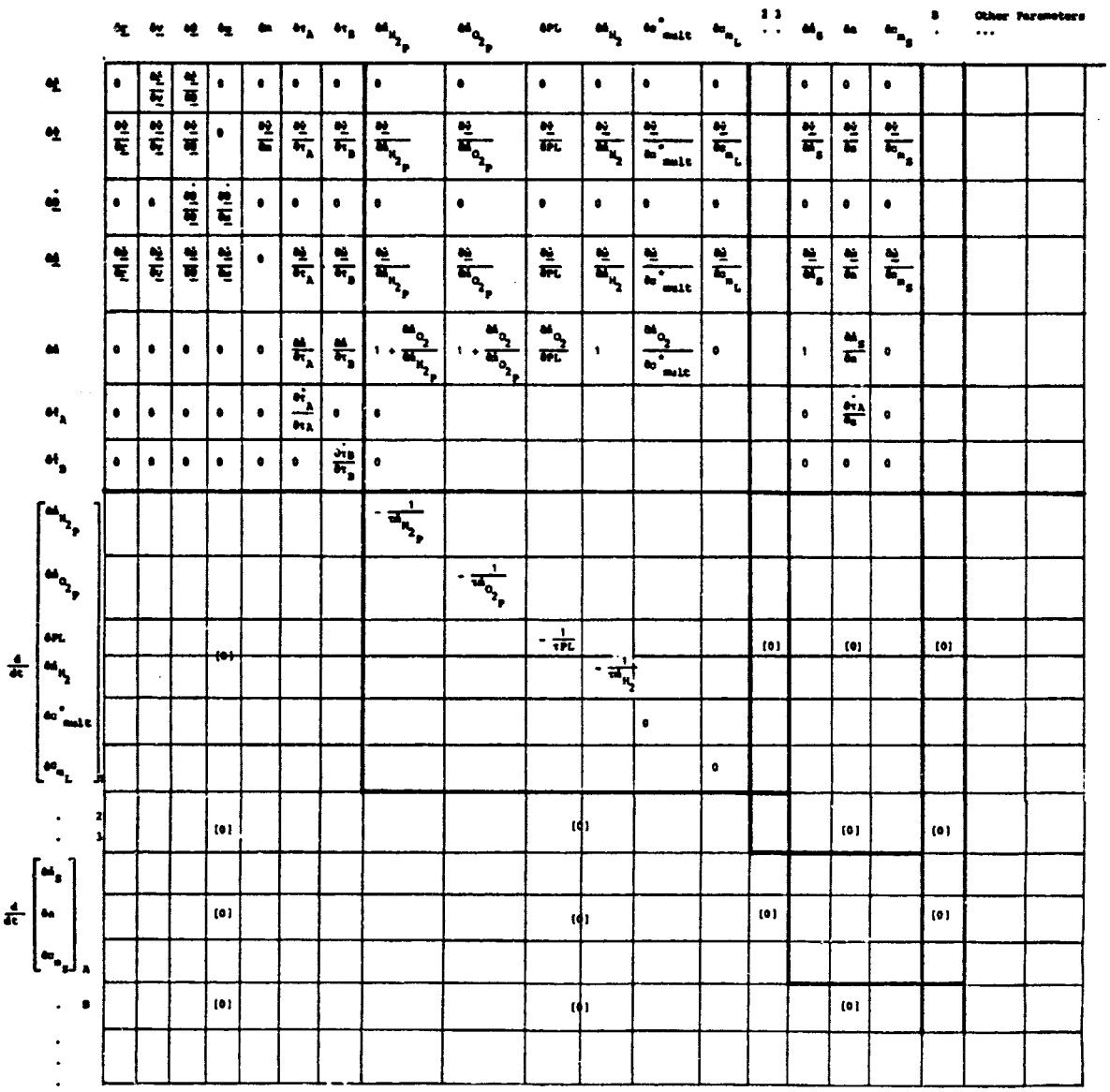

FIGURE 4.0-1. Linearized System Matrix for Equation (3)

ORIGINAL PAGE IS
OF POOR QUALITY

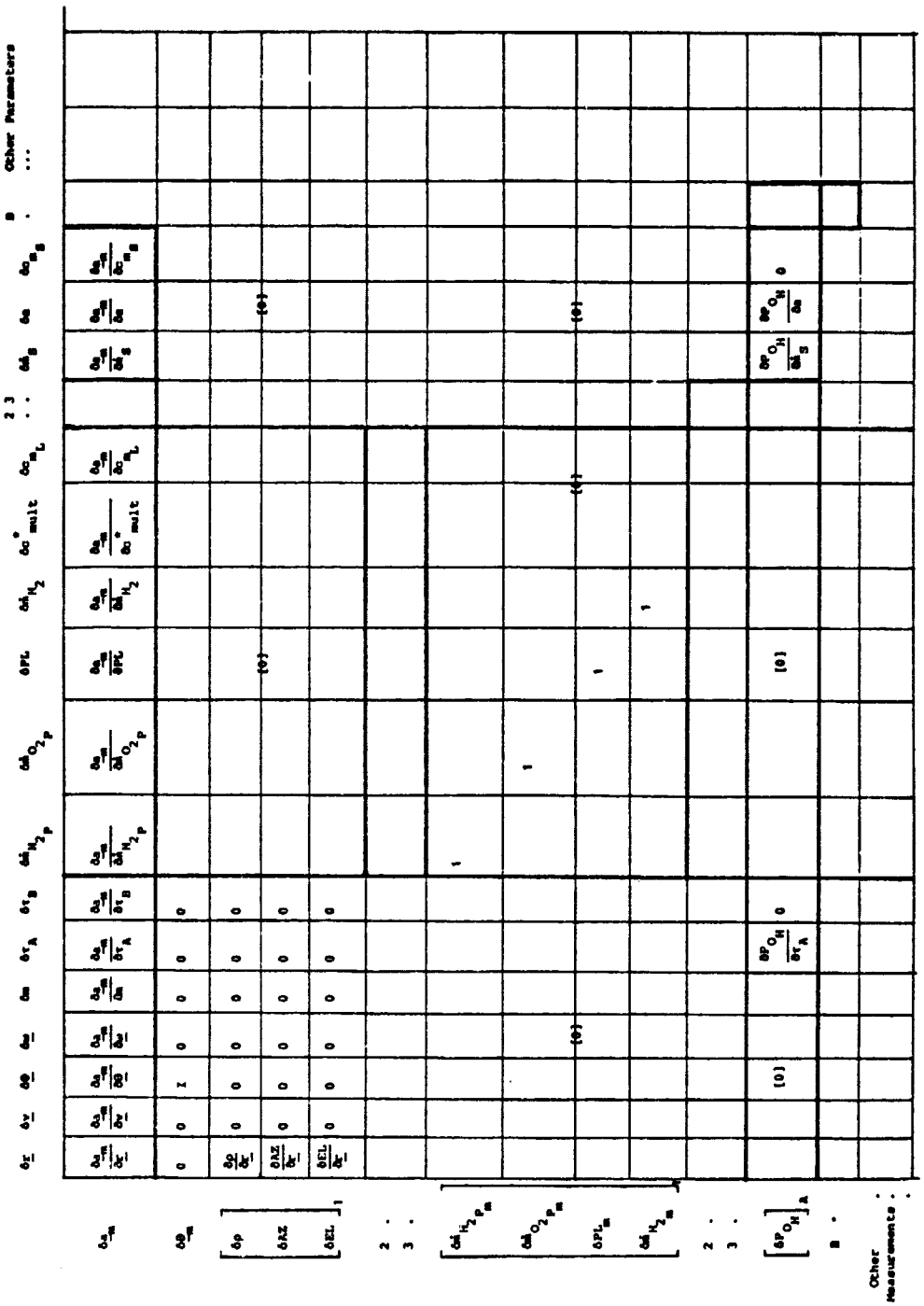

FIGURE 4.0-2. Linearized Measurement Matrix for Equation (4)

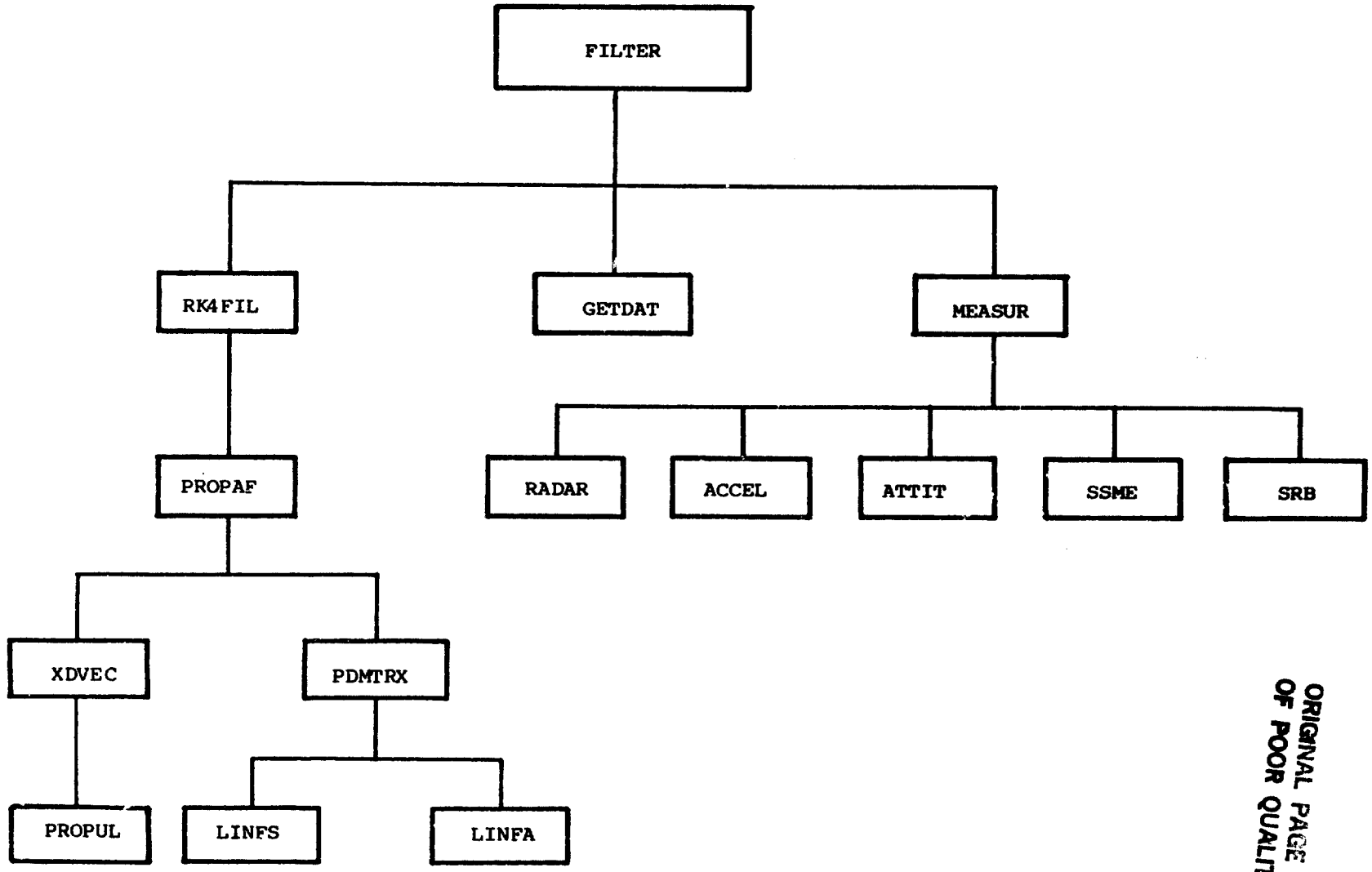

FIGURE 4.1-1. Filter Program Major Routine Linkage

TABLE 4.1-1

FILTER PROGRAM ROUTINE DESCRIPTIONS

Routine	Description
AAXES	Updates state estimates and covariances based on each accelerometer measurement - called ACCEL
ACCEL	Updates state estimates and covariances based on the accelerometer measurements - called by MEASUR
AERO	Block data routine containing dynamic aerodynamic coefficients
AEROBASE	Block data routine containing altitude dependent plume effects
AGRAV	Provides gravity vector and gradient as given in equation (45) - called by XDVEC
ATMOS	Provides atmospheric density, ambient static pressure, speed of sound, etc. based on 1962 Standard Atmosphere model - called by XDVEC
ATTIT	Updates state estimates and covariances based on the stabilized platform attitude measurements - called by MEASUR
AUXARO	Provides partial derivative of $\dot{\underline{v}}^{(B)}$, $\underline{\omega}$, and $\underline{a}_m$ with respect to $\underline{c}_f$ and $\underline{c}_m$ - called by LINFS
AUXCBI	Provides partial derivative given in Table A-1 - called by LINFS
AUXCIB	Provides partial derivative given in Table C-1 - called by LINFS
AUXINT	Provides partial derivatives of $\dot{\underline{\omega}}$ with respect to principal and cross products of inertia given in equations (74) thru (78) - called by LINFA
AUXLP1	Provides partial derivative of SSME thrust with respect to SSME parameters - called by LINFA
AUXLP2	Provides partial derivative of accelerometer measurement with respect to SSME parameters - called by ACCEL

TABLE 4.1-1 (Continued)

Routine	Description
AUXRAT	Provides partial derivative of $\underline{a}_m$ with respect to $\underline{\omega}$ as given by equation (67) - called by ACCEL
AUXRCG	Provides partial derivative of $\dot{\underline{\omega}}$ and $\underline{a}_m$ with respect to $\underline{r}_{cg}$ as given by equations (68) and (69) - called by LINFA
AUXSP1	Provides partial derivatives of SRB thrust with respect to SRB parameters - called by LINFA
AUXSP2	Provides partial derivative of $\underline{a}_m$ with respect to SRB parameters - called by ACCEL
AUXTHT	Provides partial derivative of $\dot{\underline{\theta}}$ with respect to $\underline{\theta}$ as given by equation (49) - called by LINFS
AUXTLT	Provides partial derivative of $\underline{a}_m$ with respect to platform tilt error as given in equation (85) - called by ACCEL
AUXVAB	Provides partial derivatives given in Appendix B - called by LINFS
AUXVWX	Provides partial derivatives with respect to the wind vector, $\underline{v}_w$, as given in equations (79) thru (83)
BLOCKDATA	Block data routine containing static aerodynamic coefficients as contained in Appendix D
BLKDAT	Block data routine containing run-to-run varying constants
CBIMX	Provides the transformation matrix $^{I}C^{B}$ as given in equation (34)
CCLBMX	Provides the transformation matrix $^{B}C^{G}L$ as given in equation (30)
CEFLLM	Provides the transformation matrix $^{LL}C^{EF}$ as given in equation (39)
CIEFMX	Provides the transformation matrix $^{EF}C^{I}$ as given in equation (40)
CILLMX	Provides the transformation matrix $^{LL}C^{I}$

TABLE 4.1-1 (Continued)

Routine	Description
COOR	Provides the latitude, longitude and altitude above the reference earth ellipsoid model given the earth centered position vector components
CROSS	Forms the resultant vector from the vector cross product
DIAG	Forms a matrix whose diagonal elements are taken from an input vector
ECPOS	Provides the earth centered position vector given the latitude, longitude and altitude above the referenced ellipsoid earth model
EMTRX	Provides the Euler angle rate matrix as given below equation (21)
EPOLY	Forms the evaluation of a polynomial whose first element is a constant
FILTER	Main driving routine for the extended Kalman filter estimation program
GAXES	Updates state estimates and covariances based on each platform attitude measurement - called by ATTIT
GETDAT	Provides measurement data for the filtering routines - called by FILTER
IMBED	Forms a larger matrix with a smaller matrix imbedded within it
INITIL	Provides initial estimates for the states and covariances - called by XDVEC
INNER	Forms the resultant scalar from the vector inner product
INTRP1	Provides the resultant value from a linear interpolation of a one dimensional data array
LINFA	Provides the linearization of the dynamics equation with respect to the parameter state elements as given by equation (3) - called by PDMTRX
LINFS	Provides the linearization of the dynamics equation with respect to the state elements as given by equation (3) - called by PDMTRX

TABLE 4.1-1 (Continued)

Routine	Description
MASSPROP	Block data routine containing the vehicle mass properties as a function of weight overboard
MEASUR	Calls the required updating routines based on the measurements available for processing and updates states estimates and covariance as given by equations (7) thru (9)
NASSME	Provides the nominal values of thrust and $\dot{m}$, and the associated partial derivatives as a function of power level
NASSRB	Provides the nominal values of thrust $\dot{m}$ and P_{O_H} and associated partial derivatives as a function of depth of burn.
NAERO	Provides the nominal aerodynamic coefficients and slopes based on polynomial model given in Appendix D
NOMNM	Provides the nominal mass properties as a function of weight overboard
NPLUME	Provides the nominal plume force and torque
OUTER	Forms the resultant matrix from the vector outer product
PDMTRX	Provides the elements of the covariance matrix for numerical integration as given by equation (6) - called by PROPAF
PROPAF	Calls the routines providing state estimate and covariance for numerical integration - called by FILTER
PROPUL	Provides the dynamics associated with the propulsion parameter states as given in equation (5) - called by XDVEC
RADAR	Provides nominal values of range, azimuth and elevation of radar measurements for the updating routines as given in equations (35) thru (37) - called by MEASUR

TABLE 4.1-1 (Continued)

Routine	Description
RAZMTH	Updates state estimates and covariances based on radar azimuth measurement as given in equation (56) - called by RADAR
RELEVA	Updates state estimates and covariances based on radar elevation measurement as given in equation (57) - called by RADAR
RK4FIL	Numerically integrates state estimates and covariances using Runge-Kutta fourth order algorithm - called by FILTER
RRANGE	Updates state estimates and covariances based on radar range measurement as given in equation (55) - called by RADAR
SKEW	Forms a skew symmetric matrix from the elements of the input vector
SRB	Updates state estimates and covariances based on SRB head pressure measurement - called by MEASUR
SSME	Updates state estimates and covariances based on SSME measurements - called by MEASUR
TMATP	Forms transformation matrix for a second axis rotation
TMATY	Forms transformation matrix for a third axis rotation
XDVEC	Provides elements of the state estimates for numerical integration as given by equation (5) - called by PROPAF
ZEROM	Zeros out the elements of an input matrix

TABLE 4.1-2

VECTOR/MATRIX LIBRARY ROUTINES

Routine	Description
ADD	Adds two compatible vector/matrix arrays
MULT	Multiplies two compatible vector/matrix arrays
SMLT	Multiplies a vector/matrix by a scalar
SUBT	Subtracts one vector/matrix array from a compatible vector/matrix array
SWITCH	Renames a vector/matrix array leaving initial array intact
TRANS	Transposes a matrix array

four measurements of the pressurants (2), liquid hydrogen and power level for each main engine; and SRB for the head stagnation pressure measurement for each rocket booster.

Other routines provide results of various calculations and these routines are given in Table 4.1-1. A library of routines provides various repetitive operations and are given in Table 4.1-2.

4.2 SMOOTH Program Description

The smoothing program is similar to the filtering program in that input data are sequentially processed at discrete time instances. However, in this algorithm, the input data are data processed by the filtering program and the sequence is in reversed time. The program is simpler in structure and the major routines interconnection is shown in Figure 4.2-1. The data from the filtering program is read in subroutine INPUT. The propagation backwards in time of the smooth adjoint state vector and matrix is accomplished in PROPAB using a state transition matrix formed in STRANS. The smoothed states are updated in subroutine UPDATE.

The other routines used in the smoothing program are described in Table 4.2-1.

4.3 Program Checkout and Preliminary Results

The computer program, FILTER, has been checked out in a two step process. First, to establish confidence in the implementation of the equations of motion and all the required data, the program was operated in a state vector propagation forward in time or simulation mode. This mode corresponds to an ITYPE parameter value of zero. The first stage phase of flight was "simulated" with the vehicle attitude time history prescribed by the nominal attitude versus velocity commands. During this mode of operation, errors representing measurement uncertainty were added to the uncorrupted measurement values for later processing by the filter program in a ITYPE equals one mode. The results of this operation yielded an input file, INPUT.DAT, as presented in Volumn II.

For the initial checkout, only measurement errors were included for the filter program checkout. With these being the only errors, estimates produced by the filter program should be zero or very small. Since these estimates are random variables, the mean value of these estimates should also be zero, however, this was not quantitatively evaluated in the initial checkout.

Using the data generated in the simulation mode, the filter program was checked out. The objective in checking the program out is to evaluate several attributes of the system model and the significance of the measurements. The system model formulated should provide adequate sensitivity of the state elements to the error parameters included in the model (reachability). Also, via measurements are estimates of the error parameters produced with continually modified uncertainty (observability). The uncertainty of the errors should become smaller with each additional measurement update sequence for the estimates to converge to their

appropriate values. These attributes result from the structural properties of the system model and measurements and could be evaluated by more formal processes, however, due to the size and complexity of the problem here, qualitative observations of the filter's operation will be used to illustrate these properties.

The data from the example output listing FILTER.DAT in Volume II is the basis of the discussions of the preliminary results of the filter program. These data are generated by the filter program for later processing by the smoother program.

Before discussing these data, some observations resulting from the initial attempts at operating the program are mentioned. It was discovered that the selection of state and parameter uncertainties and measurement error uncertainties is crucial to the filter program proper operation and stability. This is the result of two characteristics; the first is the fact that the extended Kalman filter algorithm's performance relies on the accuracy of the estimates produced, and the second is that the propulsion parameters produce a very strong influence on all the system state elements. This highly coupled system, while initially causing some difficulty in running the program, indicates the potential for providing good estimates for all the parameters modeled.

In the FILTER.DAT listing are presented the results for one completed measurement sequence of the program. In this listing are the results of updates from two radars (RADAR), three axes of acceleration (ACCEL), and attitude (ATTIT), four measurements for each of the three main engines (SSME) and the measurement from each of the two solid rocket boosters (SRB). Output for each measurement are: the 39 state estimate values, the 39 diagonal elements of the estimation error covariance matrix, the value of

the residual (difference between the measurement and the estimate of the measurement formed from the state estimates) and the inverse of the quantity $(H^T P_K(+)H + R)$ - a scalar, and 39 values of the appropriate row of the linearized measurement matrix presented in Figure 4.0-2. For initial checkout purposes, the update interval was selected as one-tenth of a second for all the measurements. This interval can be later modified as appropriate for each measurement processed.

Scanning the state estimates produced by the filter shows that as a result of each measurement, the values of the states are modified by the measurement update. The significance of the measurement is reflected by the reduced estimate uncertainty as quantified by the change in the estimate error variance reduction. After propagation up to the measurement time, it is seen from the data that the most significant measurements for the propulsion parameter elements 16 through 39 are the accelerometer, SSME, and SRB measurements. However, the radar and attitude measurements also produce reduced estimation error variances in these parameters in addition to the main state elements of position, velocity, attitude, etc. The significance of this is the ability to provide estimates of biases in the accelerometer, SSME and SRB if present. Also of significance is the fact that SSME measurement updates reduce uncertainty in SRB parameters and visa versa. This is again the result of the highly coupled system model and measurements. The individuality of the three SSME's parameter estimates is maintained by the filter. This is contributed to by the structural deformation values used since the SSME gimbal angles used are the nominal cant angles. This can be seen in the accelerometer updates. The final point to emphasize is the ability to reduce the uncertainty of the vehicle mass. This is the result of the accelerometer, SSME and SRB measurements.

These preliminary results indicate the possibility of the filter being able to provide estimates of the propulsion parameters from either the accelerometer or SSME and SRB measurements, and certainly from both.

Continued running of the filter with several more measurement update times showed continued improvement (reduction) of the estimation error covariance. However, after approximately 5 updates, some of the diagonal elements of the estimation error covariance became negative which is an indication of filter divergence. This problem can be rectified by proper selection of initial values for the state and parameter error covariances and selection of measurement error levels. This "tuning" process should be done using real data rather than synthetic data.

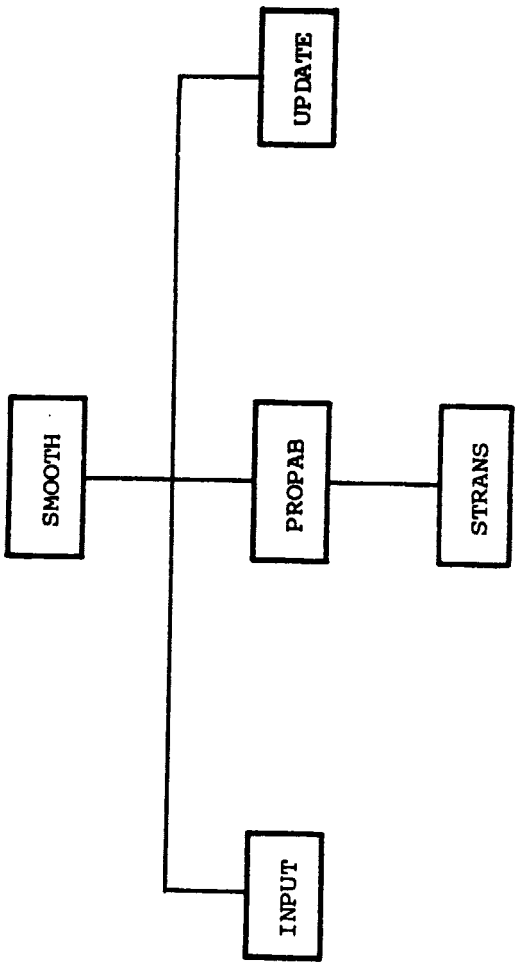

FIGURE 4.2-1. Smooth Program Major Routine Linkage

TABLE 4.2-1

SMOOTH PROGRAM ROUTINE DESCRIPTIONS

Routine	Description
IMBED	Forms a larger matrix with a smaller matrix imbedded within it
INPUT	Provides the inputs to the smoother algorithm in reverse time - called by SMOOTH
LITINI	Provides initial values for smoother algorithm which are final values from filter algorithm - called by SMOOTH
OUTER	Forms the resultant matrix from the vector outer product
PROPAB	Propagates smoother states and covariances backwards in time to next previous measurement time using state transition matrix as given in equations (18) and (19) - called by SMOOTH
SMOOTH	Main driving routine for the modified Bryson-Frazier smoothing algorithm
STRANS	Provides the state transition matrix based or the linearized state matrix, $F(\hat{x}(t), t)$, as given in equation (12) - called by PROPAB
UPDATE	Provides smoother state estimates and covariance updates as given by equations (14) thru (17) - called by SMOOTH

REFERENCES

1. Sage, A. P., Optimum Systems Control, Prentice-Hall, Inc., Englewood Cliffs, N. J., 1968.

2. Bierman, G. J., "Fixed Interval Smoothing with Discrete Measurements," Int. Jr. Control, Vol. 13, No. 1, 1975, pp. 65-75.

3. Jazwinski, A. H., Stochastic Processes and Filtering Theory, Academic Press, New York, 1970.

4. Davis, L. D., "Coordinate Systems for the Space Shuttle Program," NASA TMX-58153, October, 1974.

5. Perry, E. L., "Quaternions and Their Use," NASA/JSC Internal Note 82-FM-64, December, 1982.

6. Lear, W. M., "Description of the LRBET Program," NASA/JSC Internal Note 81-FM-5, February, 1981.

7. Hill, P. G. and Peterson, C. R., Mechanics and Thermodynamics of Propulsion, Addison-Wesley, Reading, Massachusetts, 1965.

8. Redus, J. R., Private communication.

APPENDIX A

PARTIAL DERIVATIVE OF THE VECTOR ${}^{I}_{C}{}^{B}\underline{v}$ wrt $\underline{\theta}$

This partial derivative is one of several that occurs frequently in the formulation of the linearized system state and measuremetn eqautions. The desired partial derivative is

$$\frac{\partial}{\partial \underline{\theta}} \begin{bmatrix} (\cos\theta\cos\psi)v_1 + (\substack{\sin\phi\sin\theta\cos\psi \\ -\cos\phi\sin\psi})v_2 + (\substack{\cos\phi\sin\theta\cos\psi \\ +\sin\phi\sin\psi}) v_3 \\ (\cos\theta\sin\psi)v_1 + (\substack{\sin\phi\sin\theta\sin\psi \\ +\cos\phi\cos\psi})v_2 + (\substack{\cos\phi\sin\theta\sin\psi \\ -\sin\phi\cos\psi}) v_3 \\ (-\sin\theta)v_1 + (\sin\phi\cos\theta)v_2 + (\cos\phi\cos\theta)\, v_3 \end{bmatrix} \quad \text{A-1}$$

The resulting matrix is given in Table A-1.

TABLE A-1. Partial Derivative of $^{I}C^{B}\,\underline{v}$ wrt θ

$-\sin\theta\cos\psi\ v_1$	$-\cos\theta\sin\psi\ v_1$	
$+\sin\varphi\cos\theta\cos\psi\ v_2$	$-(\sin\varphi\sin\theta\sin\psi + \cos\varphi\cos\psi)v_2$	$(\cos\varphi\sin\theta\cos\psi + \sin\varphi\sin\psi)v_2$
$+\cos\varphi\cos\theta\cos\psi\ v_3$	$-(\cos\varphi\sin\theta\sin\psi - \sin\varphi\cos\psi)v_3$	$-(\sin\varphi\sin\theta\cos\psi - \cos\varphi\sin\psi)v_3$
$-\sin\theta\sin\psi\ v_1$	$\cos\theta\cos\psi\ v_1$	
$+\sin\varphi\cos\theta\sin\psi\ v_2$	$+(\sin\varphi\sin\theta\cos\psi - \cos\varphi\sin\psi)v_2$	$(\cos\varphi\sin\theta\sin\psi - \sin\varphi\cos\psi)v_2$
$+\cos\varphi\cos\theta\sin\psi\ v_3$	$+(\cos\varphi\sin\theta\cos\psi + \sin\varphi\sin\psi)v_3$	$-(\sin\varphi\sin\theta\sin\psi + \cos\varphi\cos\psi)v_3$
$-\cos\theta\ v_1$	0	$\cos\varphi\cos\theta\ v_2$
$-\sin\varphi\sin\theta\ v_2$		$-\sin\varphi\cos\theta\ v_3$
$-\cos\varphi\sin\theta\ v_3$		

APPENDIX B

$\frac{\partial v_m}{\partial \underline{v}^{(B)}}$, $\frac{\partial \alpha}{\partial \underline{v}^{(B)}}$, $\frac{\partial \beta}{\partial v^{(B)}}$, $\frac{\partial \alpha}{\partial h}$, $\frac{\partial \beta}{\partial h}$ and $\frac{\partial v_m}{\partial h}$ Expressions

These partial derivatives occur frequently and will be developed in this appendix. The equation for $\underline{v}_r$ is

$$\underline{v}_r = \underline{v}^{(B)} - B_C{}^{LL}\, \underline{v}_w^{(LL)} \qquad \text{B-1}$$

Since the wind velocity, $\underline{v}_w^{(LL)}$, is only a function of altitude then

$$\frac{\partial}{\partial \underline{v}_r} = \frac{\partial}{\partial \underline{v}^{(B)}} \, . \qquad \text{B-2}$$

The first partial derivative, $\frac{\partial v_m}{\partial \underline{v}^{(B)}}$, is

$$\frac{\partial v_m}{\partial \underline{v}^{(B)}} = \frac{1}{v_m} \begin{bmatrix} v_{r_1} \\ v_{r_2} \\ v_{r_3} \end{bmatrix}^T \, . \qquad \text{B-3}$$

The second, $\frac{\partial \alpha}{\partial \underline{v}^{(B)}}$, is given by

$$\frac{\partial \alpha}{\partial \underline{v}^{(B)}} = \begin{bmatrix} \dfrac{-v_{r_3}}{v_{r_1}^2 + v_{r_3}^2} \\ 0 \\ \dfrac{v_{r_1}}{v_{r_1}^2 + v_{r_3}^2} \end{bmatrix}^T \qquad \text{B-4}$$

The equation for $\dfrac{\partial \beta}{\partial \underline{v}^{(B)}}$ is

$$\frac{\partial \beta}{\partial \underline{v}^{(B)}} = \begin{bmatrix} \dfrac{-v_{r_1} v_{r_2}}{v_m^3 \sqrt{v_{r_1}^2 + v_{r_3}^2}} \\ \dfrac{\sqrt{v_{r_1}^2 + v_{r_3}^2}}{v_m^3} \\ \dfrac{-v_{r_2} v_{r_3}}{v_m^3 \sqrt{v_{r_1}^2 + v_{r_3}^2}} \end{bmatrix}^T \qquad \text{B-5}$$

The following equations define the last three required partial derivatives

$$\frac{\partial \alpha}{\partial h} = - \frac{\partial \alpha}{\partial \underline{v}^{(B)}} \; B_C{}^{LL} \; \frac{\partial \underline{v}_w^{(LL)}}{\partial h} \qquad \text{B-6}$$

$$\frac{\partial \beta}{\partial h} = - \frac{\partial \beta}{\partial \underline{v}^{(B)}} \; B_C{}^{LL} \; \frac{\partial \underline{v}_w^{(LL)}}{\partial h} \qquad \text{B-7}$$

$$\frac{\partial v_m}{\partial h} = - \frac{\partial \beta}{\partial \underline{v}^{(B)}} \; B_C{}^{LL} \; \frac{\partial \underline{v}_w^{(LL)}}{\partial h} \qquad \text{B-8}$$

APPENDIX C

PARTIAL DERIVATIVE OF THE VECTOR ${}^{B}C^{I}\,\underline{v}$ wrt $\underline{\theta}$

The third of the frequently occurring required partial derivatives is

$$\frac{\partial}{\partial \underline{\theta}} \begin{bmatrix} \cos\theta\cos\psi\, v_1 & + & \cos\theta\sin\psi\, v_2 & - & \sin\theta\, v_3 \\ (\substack{\sin\phi\sin\theta\cos\psi \\ -\cos\phi\sin\psi})v_1 & + & (\substack{\sin\phi\sin\theta\sin\psi \\ +\cos\phi\cos\psi})v_2 & + & \sin\phi\cos\theta\, v_3 \\ (\substack{\cos\phi\sin\theta\cos\psi \\ +\sin\phi\sin\psi})v_1 & + & (\substack{\cos\phi\sin\theta\sin\psi \\ -\sin\phi\cos\psi})v_2 & + & \cos\phi\cos\theta\, v_3 \end{bmatrix} \qquad \text{C-1}$$

The resulting matrix is given in Table C-1.

TABLE C-1. Partial Derivative of ${}^{B}C^{I}\,\underline{v}$ wrt $\underline{\theta}$

0	$-\sin\theta\cos\psi\ v_1$ $-\sin\theta\sin\psi\ v_2$ $-\cos\theta\ v_3$	$-\cos\theta\sin\psi\ v_1$ $+\cos\theta\cos\psi\ v_2$
$(\cos\phi\sin\theta\cos\psi + \sin\phi\sin\psi)v_1$ $-(\cos\phi\sin\theta\sin\psi - \sin\phi\cos\psi)v_2$ $+\cos\phi\cos\theta\ v_3$	$\sin\phi\cos\theta\cos\psi\ v_1$ $+\sin\phi\cos\theta\sin\psi\ v_2$ $-\sin\phi\sin\theta\ v_3$	$-(\sin\phi\sin\theta\sin\psi + \cos\phi\cos\psi)v_1$ $+(\sin\phi\sin\theta\cos\psi - \cos\phi\sin\psi)v_2$
$-(\sin\phi\sin\theta\cos\psi - \cos\phi\sin\psi)v_1$ $-(\sin\phi\sin\theta\sin\psi + \cos\phi\cos\psi)v_2$ $-\sin\phi\cos\theta\ v_3$	$\cos\phi\cos\theta\cos\psi\ v_1$ $+\cos\phi\cos\theta\sin\psi\ v_2$ $-\cos\phi\sin\theta\ v_3$	$-(\sin\phi\sin\theta\cos\psi - \cos\phi\sin\psi)v_1$ $+(\cos\phi\sin\theta\cos\psi + \sin\phi\sin\psi)v_2$

APPENDIX D

AERODYNAMIC MODELING REGRESSION ANALYSIS AND RESULTS

The aerodynamic data tables provided as IVBC3 data has been incorporated into an aerodynamic coefficient polynomial model. This modeling effort reduces the dimensionality of the numerical tables to one and reduces the storage requirements for the aerodynamic model.

The coefficient model used for the two stages differ slightly as a result of the available data. The regression analysis led in the selection of the form of the aerodynamic model. Terms with insignificant correlation were eliminated from the model.

In equation form, the first stage static coefficients of axial force, C_A; normal force, C_N; pitching moment, C_m; rolling moment, C_ℓ; side force, C_Y; and yawing moment, C_n; are given below

$$C_A = C_{A_o} + C_{A_\alpha}\,\alpha + C_{A_{\alpha^2}}\,\alpha^2 + C_{A_{\alpha\beta^2}}\,\alpha\beta^2 + C_{A_{\beta^2}}\,\beta^2 \qquad \text{D-1}$$

$$C_N = C_{N_o} + C_{N_\alpha}\,\alpha + C_{N_{\alpha\beta^2}}\,\alpha\beta^2 \qquad \text{D-2}$$

$$C_m = C_{m_o} + C_{m_\alpha}\,\alpha + C_{m_{\alpha\beta^2}}\,\alpha\beta^2 \qquad \text{D-3}$$

$$C_\ell = C_{\ell_o} + C_{\ell_\beta}\,\beta + C_{\ell_{\alpha\beta}}\,\alpha\beta + C_{\ell_{\alpha^2\beta}}\,\alpha^2\beta \qquad \text{D-4}$$

$$C_Y = C_{Y_o} + C_{Y_\beta}\,\beta + C_{Y_{\alpha\beta}}\,\alpha\beta + C_{Y_{\alpha^2\beta}}\,\alpha^2\beta \qquad \text{D-5}$$

$$C_n = C_{n_o} + C_{n_\beta}\,\beta + C_{n_{\alpha\beta}}\,\alpha\beta + C_{n_{\alpha^2\beta}}\,\alpha^2\beta \qquad \text{D-6}$$

The corresponding second stage model is given by the following equations

$$C_A = C_{A_o} + C_{A_\alpha}\,\alpha + C_{A_{\alpha^2}}\,\alpha^2 \qquad \text{D-7}$$

$$C_N = C_{N_o} + C_{N_\alpha}\,\alpha + C_{N_{\alpha^2}}\,\alpha^2 \qquad \text{D-8}$$

$$C_m = C_{m_o} + C_{m_\alpha}\,\alpha + C_{m_{\alpha^2}}\,\alpha^2 \qquad \text{D-9}$$

$$C_\ell = C_{\ell_o} + C_{\ell_\beta}\,\beta + C_{\ell_{\alpha\beta}}\,\alpha\beta + C_{\ell_{\alpha^2\beta}}\,\alpha^2\beta \qquad \text{D-10}$$

$$C_Y = C_{Y_o} + C_{Y_\beta}\,\beta + C_{Y_{\alpha\beta}}\,\alpha\beta + C_{Y_{\alpha^2\beta}}\,\alpha^2\beta \qquad \text{D-11}$$

$$C_n = C_{n_o} + C_{n_\beta}\,\beta + C_{n_{\alpha\beta}}\,\alpha\beta + C_{n_{\alpha^2\beta}}\,\alpha^2\beta \qquad \text{D-12}$$

For the first stage, data from an angle-of-attack range of -6 to +6 degrees was used in the regression analysis. Data from a range of -8 to +4 degrees was used for the second stage. The results, TCXX..., from the regression analysis is presented below for each of the coefficients, $C_{XX...}$, above.

TABLE D-1. First Stage Axial Force Coefficient

PROBLEM SET: CAFA

MACH #	TCA0	TCAA	TCAAB2	TCAB2	T CAA2
.6	0.14888462	-0.14939267E-02	0.52950736E-05	-0.19513888E-03	-0.36778764E-03
.8	0.14096716	-0.16073198E-02	0.80431100E-05	-0.15666662E-03	-0.29035713E-03
.9	0.15895303	-0.87178504E-03	-0.79241381E-05	-0.10849207E-03	-0.17375973E-03
.95	0.18570921	-0.80946332E-03	-0.97817874E-05	-0.14827383E-03	-0.22280747E-03
1.0	0.24431951	-0.68517815E-03	-0.85392085E-05	-0.20781747E-03	-0.32113091E-03
1.1	0.25983587	-0.53749926E-03	0.31472900E-05	-0.17412701E-03	-0.28126000E-03
1.15	0.26992825	-0.20928589E-03	-0.46378850E-05	-0.13521819E-03	-0.23748010E-03
1.25	0.28716668	-0.47267828E-03	-0.17535077E-05	-0.12434516E-03	-0.26166640E-03
1.4	0.30411604	-0.53303648E-03	-0.35093940E-05	-0.19692448E-03	-0.16787715E-03
1.55	0.30857432	-0.51839335E-03	-0.30256535E-05	-0.21642850E-03	-0.12068918E-03
1.8	0.30735463	-0.11330346E-02	0.91515847E-05	-0.18192461E-03	-0.79305413E-04
2.2	0.28761023	-0.97124977E-03	-0.10002519E-04	-0.89146888E-04	-0.40277255E-05
2.5	0.28410554	-0.12258916E-02	-0.14255994E-04	-0.38432758E-04	0.16438302E-04
3.5	0.28069707	-0.27267837E-02	-0.18130060E-04	0.14365064E-03	0.11210326E-03
4.5	0.28001353	-0.40642847E-02	-0.13194465E-04	0.15932534E-03	0.14424580E-03

TABLE D-2. First Stage Normal Force Coefficient

PROBLEM SET: CNFA

MACH #	TCN0	TCNA	TCNAB2
.6	0.06175191	0.47317315E-01	-0.34952373E-06
.8	0.08705191	0.51266242E-01	-0.21971118E-04
.9	0.06880905	0.55013947E-01	0.37438092E-05
.95	0.06304239	0.55984642E-01	0.12846999E-04
1.0	0.05150905	0.57926252E-01	0.31073960E-04
1.1	0.04629619	0.58463752E-01	0.18769655E-04
1.15	0.05327953	0.56734987E-01	0.49979085E-05
1.25	0.06288191	0.56824278E-01	0.19573376E-04
1.4	0.05508667	0.56935535E-01	0.44349854E-04
1.55	0.04784143	0.56824278E-01	0.24865894E-04
1.8	0.02033000	0.57594139E-01	-0.13175871E-04
2.2	-0.00378286	0.52612297E-01	0.82223523E-05
2.5	-0.03606287	0.51134817E-01	0.49027673E-04
3.5	-0.04565714	0.39903577E-01	0.62995699E-04
4.5	-0.05337614	0.36437500E-01	0.43675380E-04

TABLE D-3. First Stage Pitching Moment Coefficient

PROBLEM SET: CMFA

MACH #	TCM0	TCMA	TCMAB2
.6	-0.08[illegible]762	-0.15543575E-01	0.16693601E-05
.8	-0.107[illegible]715	-0.18000530E-01	0.21009337E-04
.9	-0.09791238	-0.19910170E-01	0.46228233E-05
.95	-0.08543953	-0.20583043E-01	0.85657601E-04
1.0	-0.07620762	-0.21927318E-01	0.21230151E-05
1.1	-0.06862953	-0.20931607E-01	-0.26527516E-04
1.15	-0.07373904	-0.20659992E-01	0.65993113E-05
1.25	-0.07957237	-0.20311428E-01	-0.95234293E-06
1.4	-0.07712714	-0.20116061E-01	-0.17661379E-04
1.55	-0.06862857	-0.20584987E-01	0.12942927E-05
1.8	-0.05165952	-0.22142328E-01	0.42312208E-05
2.2	-0.02029048	-0.19702136E-01	-0.14325634E-04
2.5	0.00235619	-0.18991778E-01	-0.52894680E-04
3.5	0.01028095	-0.13785718E-01	-0.24528768E-04
4.5	0.01356667	-0.11521422E-01	-0.27753043E-04

TABLE D-4. First Stage Rolling Moment Coefficient

PROBLEM SET: CLLA

MACH #	TCLL0	TCLLB	TCLLAB	TCLLA2B
.6	0.00009800	-0.55153607E-02	-0.18314904E-03	0.25525271E-05
.8	-0.00100400	-0.51660468E-02	-0.24067984E-03	-0.47074923E-05
.9	0.00119100	-0.53059668E-02	-0.17415131E-03	0.40663767E-06
.95	0.00113500	-0.57055471E-02	-0.18708523E-03	0.26400435E-05
1.0	0.00107300	-0.65046088E-02	-0.21297160E-03	0.71316317E-05
1.1	0.00255850	-0.73706545E-02	0.23723571E-04	0.41424133E-04
1.15	0.00142150	-0.64209271E-02	-0.10909401E-03	0.19684549E-04
1.25	0.00088950	-0.61848979E-02	-0.15336619E-03	0.76067136E-05
1.4	0.00162650	-0.60260380E-02	-0.20835867E-03	-0.20967154E-04
1.55	0.00162500	-0.57253810E-02	-0.20703886E-03	0.41421335E-05
1.8	0.00160650	-0.55433516E-02	-0.17273379E-03	0.71404006E-05
2.2	0.00164350	-0.53707338E-02	-0.55630488E-04	0.12803971E-04
2.5	0.00175700	-0.46027126E-02	-0.66665525E-04	0.22202585E-05
3.5	0.00078500	-0.38413065E-02	-0.45428569E-04	-0.94020070E-05
4.5	-0.00035500	-0.32225023E-02	-0.65075328E-04	-0.85059000E-05

TABLE D-5. First Stage Side Force Coefficient

PROBLEM SET: CYA

MACH #	TCY0	TCYB	TCYAB	TCYA2B
.6	0.00040550	-0.34736611E-01	-0.24396958E-03	-0.34743120E-04
.8	0.00611750	-0.35624493E-01	-0.19144324E-03	-0.68390669E-04
.9	0.00208050	-0.37405483E-01	-0.96200623E-04	-0.65476504E-04
.95	0.00340600	-0.37516881E-01	-0.16656239E-03	-0.65729291E-04
1.0	0.00659450	-0.37924547E-01	-0.28471148E-03	-0.51625058E-04
1.1	0.00389250	-0.35857856E-01	-0.67672569E-04	-0.67499590E-04
1.15	0.00896900	-0.34745876E-01	-0.10685262E-03	-0.56302903E-04
1.25	0.01099600	-0.33643633E-01	-0.21200742E-03	-0.70274968E-04
1.4	0.00895500	-0.32880556E-01	-0.30565454E-03	-0.94529889E-04
1.55	0.00684850	-0.36689218E-01	-0.21161194E-03	-0.58715108E-04
1.8	0.00122250	-0.37921807E-01	0.23066868E-03	0.11196062E-04
2.2	-0.00312350	-0.39925124E-01	0.12333597E-03	-0.23788327E-04
2.5	0.00190050	-0.38449090E-01	0.28201332E-03	-0.50999923E-04
3.5	0.00643500	-0.34494311E-01	0.69754681E-03	-0.20773427E-04
4.5	0.00000500	-0.30585317E-01	0.73324196E-03	-0.23277323E-05

TABLE D-6. First Stage Yawing Moment Coefficient

PROBLEM SET: CLNA

MACH #	TCLN0	TCLNB	TCLNAB	TCLNA2B
.6	0.00101900	0.14767525E-01	0.56945679E-04	0.81995468E-05
.8	-0.00196700	0.15323062E-01	0.11934886E-03	0.30770094E-04
.9	0.00001700	0.15911508E-01	-0.12992905E-04	0.26990148E-04
.95	-0.00033150	0.16263550E-01	-0.21390285E-05	0.21246726E-04
1.0	-0.00102900	0.16967123E-01	0.19518508E-04	0.97513848E-05
1.1	-0.00056750	0.15625395E-01	0.11725974E-04	0.28817041E-04
1.15	-0.00357700	0.15465586E-01	0.40781717E-04	0.19518948E-04
1.25	-0.00415650	0.15171567E-01	0.17625467E-03	0.30797459E-04
1.4	-0.00269050	0.14852828E-01	0.32387782E-03	0.55297049E-04
1.55	-0.00395800	0.15761562E-01	0.23744810E-03	0.29008272E-04
1.8	-0.00297900	0.17182207E-01	0.21290279E-03	0.23987936E-05
2.2	-0.00073950	0.18076595E-01	0.11312054E-03	0.10975672E-04
2.5	-0.00348650	0.16406817E-01	-0.58733131E-04	0.34038654E-04
3.5	-0.00259800	0.13792288E-01	-0.43780611E-03	0.47138979E-05
4.5	0.00097000	0.11427909E-01	-0.46182974E-03	-0.30127571E-05

TABLE D-7. Second Stage Longitudinal Coefficients

PROBLEM SET: CAF2

MACH #	TCA20	TCA2A	TCA2A2
3.5	0.17786667	-0.38053570E-02	0.11815455E-03
4.5	0.16868572	-0.42267856E-02	0.16160712E-03
6.0	0.1681 476	-0.43714279E-02	0.12023804E-03
8.0	0.1732 7619	-0.46357140E-02	0.10416679E-03
10.0	0.16560951	-0.47821430E-02	0.14226201E-03

PROBLEM SET: CNF2

MACH #	TCN20	TCN2A	TCN2A2
3.5	-0.08282144	0.27379462E-01	0.24330383E-03
4.5	-0.07680953	0.24214283E-01	0.18452371E-03
6.0	-0.06490477	0.21875000E-01	0.38690865E-04
8.0	-0.06376192	0.20946428E-01	-0.32738029E-04
10.0	-0.06909525	0.20232143E-01	-0.29761522E-05

PROBLEM SET: CMF2

MACH #	TCM20	TCM2A	TCM2A2
3.5	0.03514286	-0.10821427E-01	-0.17857179E-04
4.5	0.04723810	-0.86785713E-02	0.11904769E-03
6.0	0.04276191	-0.68392851E-02	0.86309483E-04
8.0	0.03900000	-0.56071421E-02	0.89285677E-04
10.0	0.03719047	-0.50357138E-02	0.11309532E-03

>

TABLE D-8. Second Stage Lateral Coefficients

PROBLEM SET: CY2

MACH #	Y20	TCY2B	TCY2AB	TCY2A2B
3.5	-0. 283400	-0.35310987E-01	0.67670009E-03	0.41799358E-04
4.5	-0. 176067	-0.32411996E-01	0.65709988E-03	0.32219676E-04
6.0	-0.00862133	-0.28534999E-01	0.60950016E-03	0.41402013E-05
8.0	-0.01420600	-0.25360515E-01	0.55275002E-03	-0.10169592E-04
10.0	-0.01559400	-0.23243498E-01	0.48189994E-03	0.23179970E-04

PROBLEM SET: CLN2

MACH #	TCLN20	TCLN2B	TCLN2AB	TCLN2A2B
3.5	0.00310133	0.14233000E-01	-0.41310006E-03	-0.87519926E-04
4.5	0.00433133	0.11893496E-01	-0.37830003E-03	-0.43759825E-04
6.0	0.00328200	0.90009952E-02	-0.31595002E-03	0.36501278E-05
8.0	0.00237733	0.77250013E-02	-0.28525002E-03	-0.22901133E-05
10.0	0.00358800	0.71255034E-02	-0.27645013E-03	-0.23530063E-04

PROBLEM SET: CLL2

MACH #	TCLL20	TCLL2B	TCLL2AB	TCLL2A2B
3.5	-0.00099533	-0.55765007E-02	0.17604997E-03	-0.12449930E-04
4.5	-0.00212667	-0.46779984E-02	0.11775004E-03	-0.12530111E-04
6.0	-0.00141267	-0.38770009E-02	-0.11815000E-03	0.31110012E-04
8.0	-0.00262400	-0.33380005E-02	0.46599998E-04	-0.91998515E-06
10.0	-0.00266133	-0.32379995E-02	0.14849989E-04	0.11949987E-04